Decoding the Role of Secondary Motor Cortex Neuronal Ensembles during Cocaine Self-Administration: Insights from Longitudinal *in vivo* Calcium Imaging via Miniscopes

Yingying Chen[1], Haoying Fu[1], Amith Korada[1], Michal A. Lange[1], Chandrashekar Rayanki[1], Joreylis M.F. Montgomery[1], Tao Lu[1], Dongbing Lai[2], Shiaofen Fang[3], Changyong Guo[1], Yao-Ying Ma[1,4]

[1]. Department of Pharmacology and Toxicology, Indiana University School of Medicine, Indianapolis, IN 46202, USA.

[2]. Department of Medical and Molecular Genetics, Indiana University School of Medicine, Indianapolis, IN 46202, USA.

[3], Luddy School of Informatics, Computing and Engineering, Indiana University, Indianapolis, IN 46202, USA.

[4], Stark Neurosciences Research Institute, Indiana University School of Medicine, Indianapolis, IN 46202, USA.

Corresponding author: Dr. Yao-Ying Ma

Department of Pharmacology and Toxicology, Indiana University School of Medicine

635 Barnhill Drive, Indianapolis, IN 46202

Tel: 317-274-1536

Fax: 317-274-7714

Email: ym9@iu.edu

ABSTRACT

Recent findings in our lab demonstrated that the risk of cocaine relapse is closely linked to the hyperexcitability of cortical pyramidal neurons in the secondary motor cortex (M2), noticeable 45 days after cocaine intravenous self-administration (IVSA). The present study was designed to explore the underlying mechanisms of neuronal alterations in M2. Our hypothesis was that M2 neurons were affected directly by cocaine taking behaviors. This hypothesis was tested by monitoring individual neuronal activity in M2 using MiniScopes for *in vivo* Ca^{2+} imaging in C57BL/6J mice when they had access to cocaine IVSA as a reinforcement (RNF) contingent to active lever press (ALP) but not to inactive lever press (ILP). With support of our established pipeline to processing Ca^{2+} imaging data, the current study was designed to monitor M2 neuronal ensembles at the single-neuron level in real time with high temporal resolution and high throughput in each IVSA session and longitudinally among multiple IVSA sessions. Specifically, five consecutive 1-hr daily IVSA sessions were used to model the initial cocaine taking behaviors. Besides detailed analyses of IVSA events (ALP, ILP, and RNF), the data from Ca^{2+} imaging recordings in M2 were analyzed by (1) comparing neuronal activation within a daily IVSA session (i.e., the first vs. the last 15 min) and between different daily sessions (i.e., the first vs. the last IVSA day), (2) associating Ca^{2+} transients with individual IVSA events, and (3) correlating Ca^{2+} transients with the cumulative effects of IVSA events. Our data demonstrated that M2 neurons are exquisitely sensitive to and significantly affected by concurrent operant behaviors and the history of drug exposure, which in turn sculpt the upcoming operant behaviors and

the response to drugs. As critical nodes of the reward loop, M2 neurons appear to be the governing center orchestrating the establishment of addiction-like behaviors.

KEY WORDS

cocaine, drug taking, secondary motor cortex, miniScope, in vivo Ca^{2+} imaging

INTRODUCTION

Substance use disorder (SUD) causes a significant burden on individuals and societies globally. It is estimated that 11 million people die each year due to SUD, which is more than the number of deaths from all types of cancer[1-3]. It is well accepted that SUD is characterized by compulsive substance use, which progresses through three distinct stages: initial drug exposure, drug-free period, and relapse to the initially used substance. Although extensive efforts in SUD research have been made to unveil the neuronal mechanisms underlying relapse, which is the primary challenge of SUD patients in a clinical setting, no effective therapies to prevent relapse have been successfully established. In a previous study we demonstrated that the secondary motor cortex (M2) is a novel and critical region underlying addiction[4]. Hyperexcitability of M2 neurons increases the risk of cocaine relapse, even after a prolonged withdrawal period. This neuronal alteration was proposed be the consequence of initial cocaine exposure. Thus, we hypothesized that this initial cocaine taking experience directly affected M2.

The most reliable procedure for mimicking human SUD in laboratory animals is intravenous self-administration (IVSA) of the drug[5-10]. Traditional addiction research typically reports only the total number of IVSA events. These include active lever press (ALP) that immediately trigger reinforcement (RNF). It also accounts for inactive lever press (ILP) which has no contingent consequence. Repeat drug taking behaviors in IVSA are experience dependent. Each IVSA event (i.e., ALP, ILP, and RNF) has the potential to remodel neuronal circuits which, in turn, induces adaptations affecting the response to the next IVSA event. The interval between two adjacent IVSA events or

between two IVSA sessions may provide a consolidation time window for the brain to reorganize the experience-induced changes and be prepared to coordinate the upcoming behavioral output. Various *in vivo* recording techniques in addiction models have been used previously[11]. For example, fiber photometry can detect Ca^{2+} field changes efficiently at low cost, and fast-scan cyclic voltammetry can detect neurotransmitter release with high temporal resolution, but both lack single neuron resolution. Immediate early gene (e.g., C-fos) activation labels neurons with high spatial resolution but low temporal resolution. Benefited from the advances in imaging technology and progress in fluorescent Ca^{2+} indicators[12-14], *in vivo* Ca^{2+} imaging, which provides both high spatial and temporal resolution with high throughout in detecting individual neuronal activity, has been used in addiction research. However due to technical challenges related to Ca^{2+} imaging during IVSA (e.g., potential interference between the IV line for the IVSA procedure and the miniScope coax cable, head immobilization when the multiphoton microscopy is used), the application of *in vivo* Ca^{2+} imaging recordings in addiction models has been limited to oral self-administration, passive injections, or head-fixed animals[15-17]. Considering the precise dosing and accurate timing of the IVSA and its high validity when animals are fully awake and freely moving[18], we established a dual-channel commutator system (Doric) which allowed us to collect *in vivo* Ca^{2+} imaging data when the animals were allowed to operantly take drugs during the IVSA procedure. Together with our well-established pipeline in processing the Ca2+ imaging data, the current study was able to monitor single-neuron activation in real time with high temporal solution and high throughout in each IVSA session, as well as longitudinally across multiple IVSA sessions. Specifically, five 1-hr

daily IVSA sessions were used to model the initial cocaine taking behaviors. Besides high temporal resolution analyses of IVSA events (Fig. 1), the data from Ca^{2+} imaging recordings in M2 were analyzed by (1) comparing different time blocks within the daily IVSA session (i.e., the first vs. the last 15 min) and between different daily sessions (i.e., the first vs. the last IVSA day) (**Fig. 2**), (2) associating Ca2+ activity with an IVSA event (ALP, ILP, or RNF) (**Figs. 3-5, S1-6**), and (3) correlating this activity with the cumulative effects of IVSA events (**Figs. 6-8, S7**).

MATERIALS AND METHODS

Experimental Subjects

All procedures were performed in accordance with the United States Public Health Service Guide for Care and Use of Laboratory Animals and were approved by the Institutional Animal Care and Use Committee at Indiana University School of Medicine. Eighteen 5-week-old male C57BL/6 were purchased from the Jackson Laboratory and group housed for 5-7 days when they started surgery and behavioral procedures (Fig. 1A) during which they are singly housed. Mice were housed on a 12-hour light/dark cycle with free access to chow and water in home cage.

Surgical procedures:

(1) Microinjection of AAV

Mice were anesthetized with 2.5% isoflurane for induction and maintained with around 1.2%. A 28-gauge injection needle was used to unilaterally inject 0.5 μl/site (0.1 μl/min)

of the AAV1-Syn-jGCaMP8f-WPRE or AAV1-CaMKIIa-jGCaMP8f-WPRE solution via a Hamilton syringe into the M2 (in mm: AP, +1.80; ML, ±0.60; DV, -1.30 for M2), using the Pump 11 Elite Syringe Pumps (Harvard Apparatus). Injection needles were left in place for 5 min following injection.

(2) Lens implantation: A couple of minutes after withdrawing the AAV injection needle, objective GRIN lenses (Inscopix Inc, #1050-004595, Diameter: 1.0 mm; Lens length: ~4.0 mm; Working Distance: 0 μm-200 μm) were lowered through the cranial window to 200 μm above the center of the virus injection site. The open space between the lens' side and the skull opening was sealed by surgical silicone (Kwik-Sil) and secured by dental cement (C&B Metabond). The exposed part of the lens above the skull was further coated with black cement (Lang Dental Mfg. Co.' Inc.).

(3) Catheter implantation: 3~4 weeks later, catheter implantation was made as described previously[19-23] . Briefly, a silastic catheter was inserted into the right jugular vein, and the distal end was led subcutaneously to the back between the scapulae. Catheters were constructed from silastic tubing (length, 55 mm; inner diameter, 0.3 mm; outer diameter, 0.6 mm) connected to a One Channel Vascular Access Button™ for Mice (Instech Labs). Aluminum VABM1C cap (Instech Labs) was attached to protect the button. The catheter was flushed daily after its implantation with 1 ml/kg body weight of heparin (10 U/ml) and gentamicin antibiotic (5 mg/ml) in sterile saline to help protect against infection and catheter occlusion.

(4) Base plating: Post the catheter implantation, the mouse was maintained anesthetized with isoflurane. The cement on the top of the GRIN lens was safely removed by drill bits until the lens was exposed. The top of the lens was cleaned by lens paper with lens cleaning solution. Thereafter, a metal baseplate was mounted to the skull over the lens with Loctite super glue gel control, guided by a MiniScope for optimal field of view. After the baseplate was securely mounted, the MiniScope was taken off, a cap was attached to the baseplate and the mouse was returned to the home cage.

(5) Verification of AAV expression and the lens location: After the compliment of the behavioral test, M2-containing coronal slices of 50-μm thickness were prepared as described in the section preparing slices for patch clamp recordings, then fixed in 4% Paraformaldehyde (PFA) for no less than a couple of hours. After a brief rinse by PBS, slices were mounted with Prolong™ Gold antifade mounting reagent with DAPI (Invitrogen, Cat# P36931). Confocal imaging was performed using a Zeiss LSM 800 confocal microscope. The images were analyzed using Imaris 9.7.2 (Oxford Instruments). The animals included in this study were all approved with (a) highly enriched AAV expression in neurons, most like the pyramidal neurons, within-M2 viral injection site, and (b) the footprint of the GRIN lens tip at the top of M2 (**Fig. 2A**)

Open field test

~6 days after the catheter implantation, Black Plexiglas of testing chamber (Maze Engineers) was 60 cm for both side-widths x 50 cm in height with a floor illumination at

~60 *lux* [24]. Mice were placed in the peripheral area facing one of the randomly assigned sidewalls and then allowed to freely explore the open field. Total testing time was 5 min. Behavioral videos were processed by EthoVision XT14 Software (Noldus) and the total distance traveled during the 5 min was calculated.

Intravenous Self-administration

(1) Self-administration apparatus

Experiments were conducted in operant-conditioning chambers enclosed within sound-attenuating cabinets (Med Associates). Each chamber contained two levers randomly assigned as active *vs*. inactive levers, a food dispenser, and the conditioned stimulus light (i.e., cue light) 9 cm above each lever. No lab chow or water was provided in the chambers during the training or testing sessions.

(2) Intravenous cocaine self-administration training

~7 days after catheter implantation, cocaine self-administration training began with an overnight session at 7 PM to 7 AM on the following day. The daily training session, i.e., 1 hour per day for 5 days, started on the day after. The same training protocol was used in overnight and daily sessions. Mice were placed in the self-administration chamber on a fixed ratio (FR) 1 reinforcement schedule with the house light on. Active lever presses (ALP) resulted in a cocaine infusion (0.75 mg/kg over ~2 sec) and illumination of a cue light above the active lever for 20 sec with the house light off. In contrast, the inactive lever presses (ILP) led to no outcome but were also recorded. Rats that received at least 60 cocaine rewards in the overnight session were allowed to move to daily self-

administration of cocaine ~24 hr after the overnight training on an FR1 reinforcement schedule.

In vivo Ca^{2+} imaging recording during cocaine self-administration

Mice were habituated with the *in vivo* Ca^{2+} recording procedure by mounting the miniScope V4 (OpenEphys) to the pre-anchored base plate and recording for 5 min per day at home cage for 3 days before starting the IVSA procedures. Our data presented in **Figs. 2-8, S1-S7** were collected during the 1-hr IVSA daily sessions on the first and the last IVSA training days (i.e., Day 1 and Day 5). Facilitated by the customized commutator from Doric, mice were allowed to self-administer cocaine via pre-implanted IV catheter with no interruptions from double lines (IV solution line and the miniScope coax cable) connected to mice. Data Acquisition (DAQ) box, supported by an open source, C^{++} and Open Computer Vision (OpenCV) libraries-based software, were used to collect both Ca^{2+} and behavioral video streams simultaneously controlled by the operant chamber software, MED-PC (Med Associates) via a TTL adaptor. The sampling frequency was 30 Hz.

Ca2+ imaging analyses

(1) Extraction of Ca^{2+} transient trace from the raw videos

Among multiple types of computational tools established before in extract Ca2+transients from raw videos, a Python-based analysis pipeline, i.e., Minian[25], was used in our data analyses due to its low memory demand and user friendly parameter options. In brief, there were five steps in the pipeline. First, multiple raw videos were batched loaded and passed into a *PREPROCESSING* stage, where sensor noise and background

fluorescence from scattered light are removed. Second, rigid motions of the brain is corrected by *MOTION CORRECTION*. Third, the initial spatial and temporal matrices for later steps are generated from a seed-based approach, call *SEEDS INITIALIZATION*. Fourth, the spatial footprints of cells are further refined. Fifth, the temporal signals of cells are further refined. The last two steps, the *SPATIAL UPDATE*, and the *TEMPORAL UPDATE*, as the core computational components based on CNMF algorism, were repeated as needed until satisfactory results were reached.

(2) Cell verification

Our team has developed an open-source GUI using the python package PYQT5 for cell verification and Ca2+ transient identification (more details in a manuscript in preparation by MA Lange et al.). Synchronized visualization *via* a user-friendly single window allowed us to evaluate the CNMF output comprehensively. We visualized multidimensional Ca^{2+} signals generated by CNMF variables “C” or “S”, and directly calculated by our GUI tool such as raw fluorescent signals (F), filtered fluorescent signals ($F_{filtered}$), noise, signal-to-noise ratio (SNR), and the relative change of fluorescent intensity (ΔF/F). The individual cell footprint was generated by the CNMF variable “A” on top of the raw Ca^{2+} video or the CNMF-processing Ca^{2+} video. Selection of the footprint or the cell ID from the cell ID listed achieved by CNMF was directly associated with the raw image, the processed image, the footprint, the cell ID and the Ca2+ trances. Cells was excluded if any of this information appeared artifactual. We also plotted the SNR values for each cell. Cells with low SNR values (e.g., SNR<2) were excluded unless the Ca^{2+} transients were identifiable. There

were ~2-10 % of CNMF-identified cells per recording session per animal excluded from further data analyses.

(3) Ca^{2+} Transient identification

First, we used the Ca^{2+} transient kinetics-based auto-identification tool in our newly developed GUI platform (to be published by MA Lange et al). The transient was detected by the CNMF variable "C" and the ΔF/F. Ca^{2+} transient amplitude was determined by the peak value of the ΔF/F. The minimal Ca^{2+} transient amplitude was set as ΔF/F = 1, which required that the increase of the fluorescent intensity is at least 100% from the background level. The minimal inter-transient interval was set at 45 frames or >1.5 sec. Second, we checked the Ca^{2+} trances and further adjustment was manually made to accept new Ca^{2+} transients or reject the auto-identified Ca^{2+} transients. Lastly, we established machine-learning tools by loading the data sets of Ca^{2+} traces with auto/manually identified Ca^{2+} transients for the training, validation, and testing. Briefly, two variants of Recurrent Neural Networks machine learning models (i.e., LSTM and GRU) and two versions of the Transformer model (i.e., the original model and one using local attention) were tested. Our data demonstrated that GRU-based machine learning model is highly reliable, achieving an F1 score (i.e., a statistical measure of predictive performance) of over 0.9 (e.g., F1 = 0.94). This performance was attained using a limited dataset consisting of Ca^{2+} traces from only 10-20 cells over a 15-minute window to train the machine learning model.

(4) Bin-sized Z score during a 15-min session

A bin of 30 seconds was used in preparing data for **Figs. 3-8, S1-7**. For those spanning across two adjacent 30-sec blocks, the Ca^{2+} transients were included in the 30-sec block where they started.

There readouts of the Ca^{2+} transient signals were used in their quantification in each 30-sec block:

<u>Total Ca^{2+} transients per bin</u> were calculated by the summation of the amplitude of all the Ca^{2+} transients in each 30-sec block of the observed neurons.

<u>Ca^{2+} transient frequency per bin</u> was calculated by the number of Ca^{2+} transients in each 30-sec block of the observed neurons divided by 30 sec. The unit is Hz.

<u>Ca^{2+} transients Amplitude per bin</u> was calculated by the average of the amplitude of the Ca^{2+} transients in each 30-sec block of the observed neurons.

Z score in each 30-sec block during a 15-min time window for each neuron was calculated by the following formula:

$$Z = \frac{x - \mu}{\sigma}$$

In which x is a specific Ca^{2+} transient readout (i.e., total Ca^{2+} transient, Ca^{2+} transient frequency, or Ca^{2+} transient amplitude) from an observed neuron in any of the fifteen 30-sec time blocks, μ and σ are the corresponding mean value and the standard deviation of the fifteen 30-sec blocks of the observed neuron.

(5) Bin-sized ΔZ score within 3 min before ALP/ILP or after RNF during a 15-min time window

Neuronal ΔZ score of the total Ca^{2+} transients in a 30-sec block: Using the ALP-associated ΔZ scores of the total Ca^{2+} transients in **Fig. 3 C**, **D** as examples, each ΔZ score of the total Ca^{2+} transient in a 30-sec block was calculated by the total Ca^{2+} transient Z score minus the Z score in the bin where ALP occurred. Neurons from an animal which had at least 1 ALP during a 15-min time window were included in calculating ΔZ. Assuming there were n (as the number of) ALPs during the 15-min time window (ALP#1, ALP#2, …., ALP#n), then we would have n sets of six ΔZ values for each of the six 30-sec block with 3 min before ALP. The averaged six ΔZ values within 3 min before ALP from the n sets are presented in **Fig. 3 C**, **D**, in which each row of the six blocks represented the neuronal changes of the total Ca^{2+} transients in each 30-sec block within 3 min before ALP. Similarly, the neuronal changes of the total Ca^{2+} transients in each 30-sec block within 3 min before ILP are shown in **Fig. 4 C, D**, and the neuronal changes of the total Ca^{2+} transients in each 30-sec block within 3 min after RNF are presented in **Fig. 5 C, D**.

Neuronal ΔZ score of the frequency of Ca^{2+} transients in a 30-sec block: Similar calculations as the neuronal ΔZ score of the total Ca^{2+} transients described above, the Z scores of the frequency of the Ca^{2+} transients in each of the six 30-sec blocks was used in ΔZ score quantification. Specifically, the neuronal changes of the frequency of Ca^{2+} transients in each 30-sec block within 3 min before ALP are shown in **Fig. S1 A**, **B,** the neuronal changes of the frequency of Ca^{2+} transients in each 30-sec block within 3 min before ILP are presented in **Fig. S3 A**, **B**, and the neuronal changes of the frequency of Ca^{2+} transients in each 30-sec block within 3 min after RNF are shown in **Fig. S5 A**, **B**.

Neuronal ΔZ score of the amplitude of Ca^{2+} transients in a 30-sec block: Similar calculations as the neuronal ΔZ score of the total Ca^{2+} transients described above, the Z scores of the average amplitude of the Ca^{2+} transients in each of the six 30-sec blocks was used in ΔZ score quantification. Specifically, the neuronal changes of the amplitude of Ca^{2+} transients in each 30-sec block within 3 min before ALP are illustrated in **Fig. S2 A**, **B,** the neuronal changes of the amplitude of Ca^{2+} transients in each 30-sec block within 3 min before ILP are shown in **Fig. S4 A**, **B**, and the neuronal changes of the amplitude of Ca^{2+} transients in each 30-sec block within 3 min after RNF are shown in **Fig. S6 A**, **B**.

(6) ΔZ score-based sorting of the 30-sec bin

Each of the IVSA events (i.e., ALP, ILP, RNF)-associated 30-sec blocks before ALP/ILP or after RNF are categorized as positive response if ΔZ is more than +0.1, no response if ΔZ is between -0.1 to +0.1, or negative response (if ΔZ is less than -0.1). Specifically, the ΔZ score-based sorting of the 30-sec bins are provided in panels **E-H** in **Figs. 3-5**.

(7) Neuronal ΔZ score-based neuronal sorting of the 3-min time window

The IVSA event (i.e., ALP, ILP, or RNF)-associated 3-min time window for each neuron consisted of six 30-sec blocks. The 3-min window associated with ALP or ILP, which means the 6th 30-sec block (i.e., -30 to 0 sec or -0.5 to 0 min) was the block when the ALP or ILP occurred, was categorized as (a) positive (Pos), (b) not responsive (NR), and (c) negative (Neg) if the 5th 30-sec block (i.e. -60 to -30 sec or -1 to 0.5 min) was classified as positive, no responsive, and negative, respectively. The 3-min window

associated with RNF, which means the 1st 30-sec block (i.e., 0 to 30 sec or 0 to 0.5 min) was the block when the RNF occurred, was categorized as positive (Pos) and negative (Neg) if the nearest non-no responsive 30-sec block was classified as positive and negative, respectively. The 3-min window associated with RNF was categorized as not responsive (NR) if all the five 30-sec blocks during 30 to 180 sec (i.e., 0.5 to 3 min) are sorted as no responsive.

% of animal event (i.e., ALP, ILP, or RNF)-associated neuronal population in each 15-min was calculated for each experimental mouse as below

$$\text{Pos\%} = \frac{\text{\# of event associated Pos neurons identified in the observed mouse}}{\text{Total \# of detected neurons from the observed mouse}} \times 100$$

$$\text{NR\%} = \frac{\text{\# of event associated NR neurons identified in the observed mouse}}{\text{Total \# of detected neurons from the observed mouse}} \times 100$$

$$\text{Neg\%} = \frac{\text{\# of event associated Neg neurons identified in the observed mouse}}{\text{Total \# of detected neurons from the observed mouse}} \times 100$$

Thus, Pos%+ NR%+ Neg% = 100% for each mouse. The % of ALP-associated neuronal population in saline *vs*. cocaine mice is shown in **Fig. 3I-M**. The % of ILP-associated neuronal population in saline *vs*. cocaine mice is shown in **Fig. 4I-M**. The % of RNF-associated neuronal population in saline *vs*. cocaine mice is shown in **Fig. 5I-M**.

(8) Subcategories of Pos and Neg neuronal populations

The Pos neurons were further categorized into Pos_{pure} (*i.e.*, all the five 30-sec blocks before ALP/ILP were identified as Pos, or all the 30-sec blocks after the first Pos 30-sec blocks were identified as Pos) *vs*. Pos_{mixed} (*i.e.*, at least one of the five 30-sec blocks before ALP/ILP were identified as NR or Neg, or at least one of the 30-sec blocks after the first Pos 30-sec blocks were identified as NR or Neg). Similarly, Neg neurons were also further categorized into Neg_{pure} (*i.e.*, all the five 30-sec blocks before ALP/ILP were identified as Neg, or all the 30-sec blocks after the first Pos 30-sec blocks were identified as Neg) *vs*. Neg_{mixed} (*i.e.*, at least one of the five 30-sec blocks before ALP/ILP were identified as NR or Pos, or at least one of the 30-sec blocks after the first Pos 30-sec blocks were identified as NR or Pos). The % of detected M2 neurons in each subcategory was calculated for each animal similarly. For example, ALP-associated Pos_{mixed} % for a mouse was calculated by the # of ALP-associated Pos_{mixed} neurons identified in the observed mouse divided by the total # of detected M2 neurons from the observed mouse. The % of ALP-associated neuronal sub-population (i.e., pure vs. mixed) in saline *vs*. cocaine mice is shown in **Fig. 3N-Q**. The % of ILP-associated neuronal sub-population (i.e., pure vs. mixed) in saline vs. cocaine mice is shown in **Fig. 4 N-Q**. The % of RNF-associated neuronal sub-population (i.e., pure vs. mixed) in saline vs. cocaine mice is shown in **Fig. 5 N-Q**.

(9) Linear regression analysis:

The linear regression analysis was performed between (1) the Z scores of the total Ca^{2+} transients (**Figs. 6, 7, 8A,B**), the frequency of Ca^{2+} transients (**Fig. 8C**), or the amplitude of Ca^{2+} transients (**Fig. 8C**) and (2) the # of ALP, ILP or the RNF in each of

the fifteen 30-sec blocks during a 15-min session. A linear IVSA-event (i.e., ALP, ILP, or RNF)-associated neuron (denoted as LAN) was identified when the p value of the F test for the linear regression was less than 0.05, indicated the regression is non-zero, and the p value of the Pearson correlation analysis was also less than 0.05. The # of ALP, ILP and RNF were set up in two different ways, including (1) the counts of ALP, ILP or RNF during each 30-sec block, and (2) the counts of ALP, ILP or RNF in not only the current 30-sec block but also the previous 30-sec block(s) if there was any. Thus, we performed and compared two types of linear regression analyses, named non-cumulative (nonCML) linear regression, and cumulative (CML) linear regression, respectively as shown in **Fig. 6**. Only CML linear regression-identified LANs were further analyzed in **Figs. 7, 8**.

Statistical Analysis: Data were collected from 8 saline mice and 10 cocaine mice *in vivo,* shown as mean ± SEM (except in **Fig. 2I-K** where three dashed lines split each violin plot at the quartile positions) and/or individual values from each inter-ALP-interval (**Fig. 1R-U**), each neuron (**Figs. 2C-H**), or each mouse (**Figs. 1C-K, 2K-N, 3I-Q, 4I-Q, 5I-Q, 6A-L**). Using GraphPad Prism 10, statistical significance was assessed by Student's t test (**Fig. 1B**), two-way ANOVA (**Figs. 1C-N; 3-5 I-Q; 6 A-L**), three-way ANOVA, followed by Bonferroni post-hoc tests (**Fig. 2I-N**), or simple linear aggression and Pearson correlation analysis (**Fig. 1R-U** and neuronal characterization in **Figs. 6-8**). Statistical significance was considered to be achieved if $p < 0.05$.

RESULTS

IVSA events (i.e., ALP, ILP, RNF) during the IVSA sessions

18 mice with pre-implanted GRIN lenses into M2 and a catheter into the jugular vein were randomly assigned to IVSA of saline or cocaine (**Fig. 1A**). Mice in both groups demonstrated similar distance traveled during the 5-min OF test (**Fig. 1B**), indicating their general locomotion was comparable. As expected, saline mice showed similar #s of ALP and ILP (**Fig. 1C**), whereas cocaine mice performed more on ALP, relative to ILP throughout the five 1-hr daily sessions (**Fig. 1D**). Thus, compared to saline mice, cocaine mice earned a high # of IV injections (i.e., RNFs; **Fig. 1E**). If the 1-hr daily session was divided into 4 blocks of 15 mins each, it was apparent that, different from the gradual reduction of ALP, ILP and RNF from the first to the last 15-min block on both Day 1 and Day 5 of IVSA in saline mice, cocaine mice consistently demonstrated active ALP and RNF, accompanied with a low number of ILP, throughout the four 15-min blocks on both Day 1 and Day 5 of IVSA (**Fig. 1I-N**). The cumulative probability of three featured IVSA events in **Figs. 1L-Q** revealed distinguishable time-courses of ALP and RNF, but not ILP, between saline vs. cocaine mice. Then the inter-ALP-interval (IAI; cut off at 1000 sec) was used as an example IVSA event to demonstrate more details of the time courses of IVSA behaviors (**Fig. 1R-U**). Specifically, saline mice showed linearly increases in IAI during the first 15 min on Day 1 but not Day 5, and very few or none within-1000 sec IAI occurred in the last 15 min. Differently, cocaine mice linearly increased IAI in the first 15 min on both Day 1 and Day 5, however in the last 15 min, the number of ALP events remained steady during the last 15 min on both days. Our detailed analysis of the mouse IVSA behaviors demonstrated differences of cocaine taking behaviors within the 1-hr daily session (i.e., the first vs. the last 15 min) and

between days (e.g., Day 1 *vs*. Day 5). Thereafter, the behavior-associated *in vivo* Ca^{2+} transients in M2 neurons were investigated within a 1-hr daily session and between days.

Alterations of the Ca^{2+} transients in M2 during IVSA in saline and cocaine mice

The activity of GCaMP8f-expressing M2 neurons, primarily the pyramidal projection neurons during IVSA (**Fig. 2A, B**), was monitored by quantifying the total Ca^{2+} transients by summation of the amplitude of all Ca^{2+} transients, as well as the frequency and amplitude within an assigned time window. IVSA event-based data analyses (**Fig. 2L-N**) showed decreases of the total Ca2+ transients, which was primarily attributable to reduction of the frequency, but not amplitude, of Ca^{2+} transients from the first 15-min to the last 15-min during the1hr IVSA session on both Day 1 and Day 5 in saline mice. In contrast, in cocaine mice there were increases of total Ca2+ transients, which was attributable to both frequency and amplitude of the Ca^{2+} transients on Day 1, and then stayed at high levels consistently on Day 5. Similar changes of Ca^{2+} transients, particularly their frequency, in saline *vs*. cocaine mice were also observed when neuron-based data (**Fig. 2C-H**) were analyzed, with expected higher statistical significance (**Table S1**) due to a large number (i.e., 310 - 553) of neurons per experimental condition. Our data indicate that the reduction of the non-reinforcing operant behavior (i.e., ALP and ILP in saline mice) from the early to the late stage of daily session is associated with a reduction of the frequency of Ca^{2+} transients. This reduction could be the result of M2 neuronal adaptions to the early non-reinforced operant behaviors and also the cause of less operant behaviors in the late stage of the daily sessions (**Fig. 1R**,

S). The early reinforced operant behavior (i.e., IV cocaine-associated ALP in cocaine mice) was accompanied with lower Ca^{2+} transient frequency in M2 neurons at the early stage on Day 1, but only observed in a limited time window on Day 1. A significant rebound of the Ca^{2+} transient frequency was detected at the late stage on Day 1, which was maintained at the same plateau throughout the 1-hr IVSA session on Day 5. Within the 1-hr daily session Ca^{2+} transient frequency changes on Day 1, but not on Day 5, in M2 indicates that M2 was engaged in IVSA of cocaine differently at the early *vs*. chronic drug taking.

Cocaine affected Ca^{2+} transients before ALP, but not ILP

In order to dissect the associations between the IVSA event (i.e., ALP, ILP, or RNF) and M2 Ca^{2+} transients (total transients, frequency, and amplitude), analyses of the Ca^{2+} transients within the 3 min before ALP/ILP or after RNF were performed by averaging the IVSA event-based 3-min Ca^{2+} transients within the first and the last 15 min on Day 1 and Day 5 in **Figs 3-5**. Total Ca^{2+} transients in each of the 30-sec block within-3 min before ALP/ILP-based M2 neuronal categorization disclosed a lower Pos% (41-44% as mean; the same below) and higher Neg% (53-56%) before ALP in cocaine mice, relative to that in Saline mice (Pos, 53-60%; Neg, 36-44%) (**Fig. 3A-M**), but no significant differences of Pos% (saline, 52-56%; cocaine, 43-52%) and Neg% (saline, 44-46%; cocaine, 48-56%) before ILP between saline vs. cocaine mice (**Fig.4A-M**). Further dissection of the subtypes of Pos and Neg neurons in M2 identified that the decreases of Pos% before ALP in cocaine mice was attributable to lower Pos_{pure}% in the first 15 min and lower Pos_{mixed}% in the last 15 min on both Day 1 and Day 5 (**Fig. 3N-Q**). The increases of Neg%

before ALP in cocaine mice were attributable to higher Neg_{pure}% but not Neg_{mixed}% on Day 1 and higher Neg_{mixed}% but not Neg_{pure}% on Day 5. Interestingly, the within-session fluctuation of Pos_{pure}% and Pos_{mixed}% was observed before ALP only in saline mice and before ILP only in cocaine mice (**Fig. 4N-Q**). No fluctuations of Neg subtype neurons (Neg_{pure} and Neg_{mixed}) were observed in either saline or cocaine mice before ALP and ILP. Thus, we conclude that M2 neurons responded specifically to the cocaine-associated ALP. If the lever press has no reinforcing effects (i.e., ILP in both saline and cocaine mice), the Ca^{2+} transients before ILP are similar in saine and cocaine mice.

Cocaine IVSA affected Ca^{2+} transients after RNF

Total Ca^{2+} transients in each of the 30-sec block within-3 min after RNF-based neuronal categorization revealed that the % of Pos, NR and Neg neurons in M2 remained at a constant level within the 1-hr daily sessions on both Day 1 and Day 5 of saline IVSA, although the Ca^{2+} transients after RNF had higher Pos% (i.e., 59-64%), relative to the Neg% (i.e., 29-34%). M2 neurons in cocaine mice demonstrated lower Pos% (i.e., 32%) in the first 15 min which was then increased in the last 15 min (i.e., 49% as mean) on Day 1, and stayed at high levels in the first (58%) and the last (60%) 15 min on Day 5. On the contrary, Neg% in cocaine mice was detected with reductions on Day 1 (from the first to the last 15 min: 58% to 47%), followed by a consistent low level on Day 5 (from the first to the last 15 min: 37% to 36 %). Further dissection of the subtypes of Pos and Neg neurons in M2 in cocaine mice demonstrated that the increases of Pos% were attributable to the changes in Pos_{mixed}% but not Pos_{pure}%, and decreases of Neg% were attributable to the alteration of Neg_{pure}% but not Neg_{mixed}%. Relative to that in saline mice, the lower

Pos_{mixed}% and higher Neg_{pure}% in the first 15 min on Day 1 after cocaine IV injection may indicate the sensitivity of cocaine mice to the IV cocaine delivery at the early stage, which was altered to the level closer to that in saline mice in the last 15 min on Day 1, and then no more differences between saline vs. cocaine mice occurred throughout the 1-hr IVSA session on Day 5. The temporary but not persistent sensitivity to cocaine IV injection could be explained by the re-establishment of homeostasis in M2 after initial exposure to IV cocaine. Thus, the potential rebound of M2 neuronal response could occur during the drug withdrawal period.

Cumulative effects of IVSA events on Ca^{2+} transient activity

We would like to clarify that the Ca^{2+} transients within 3 min before ALP/ILP or after RNF-based neuronal categorization (**Figs. 3-5, S1-S6**) was done according to the ΔZ scores of Ca^{2+} transient in the six 30-sec blocks averaged from all of the IVSA events (i.e., ALP, ILP, RNF) during a 15-min time window. Thus, the sequence of the IVSA events was not ignored. Considering the drug-taking behavior is a typical experience-dependent output, we propose that the previous drug taking and drug delivery affected the upcoming neuronal activity involved in regulating impending drug taking behavior. In order to test whether M2 neurons were involved in mediating the cumulative effects of drug taking and drug delivery, using linear regression analyses, the # of ALP, ILP and RNF were set up in two different ways, including (1) the counts of ALP, ILP or RNF during each 30-sec block, and (2) the counts of ALP, ILP or RNF in not only the current 30-sec block but also the previous 30-sec block(s) if there was any. Relative to the linear analysis using non-cumulative (nonCML) # of IVSA events, we detected a larger

proportion of M2 neurons in both saline and cocaine mice, particularly in the first 15 min on both Day 1 and Day 5 when the cumulative (CML) # of ALP (**Fig. 6A**, **B**) and RNF was used (**Fig. 6I**, **J**). Furthermore, the CML # of ALP and RNF-associated increases of LAN% in M2 neurons was significantly higher in cocaine mice than saine mice (**Fig. 6C**, **D**, **K**, **L**). The CML # of ILP associated increases of the LAN% was only detected in saline mice but not cocaine mice (**Fig. 6E, F, H**). We then focused on the LANs identified by CML # of IVSA events on addressing the following two questions. First, was the increased LAN% in M2 positively or negatively associated between the Ca^{2+} influx and the IVSA event #? According to the Pearson correlation coefficient (i.e., r), our results demonstrated that, different from reduced ratio of the LAN_{Pos}% to LAN_{Neg}% associated with ALP, ILP and RNFS from the first to the last 15 min on both Day 1 and Day 5 in saline mice, cocaine IVSA increased the ratio of the LAN_{Pos}% to LAN_{Neg}% of M2 neurons associated with the ALP and RNFS, but no significant changes in the ratio of LAN_{Pos}% to LAN_{Neg}% associated with ILP (**Figs. 7**). Second, were the populations of identified LANs associated with different IVSA events (i.e., ALP, ILP, RNF) separate or overlapped? Our data (**Fig. 8A**) showed a lower proportion of overlapped LANs between those associated with ALP/RNF vs. ILP in cocaine mice, relative to that in saline mice. This separation in cocaine mice was distinct at the last 15 min but not the first 15 min on Day 1 and both 15 min sessions on Day 5, and can be primarily attributed to the frequency (**Fig. 8B**), but not the amplitude (**Fig. 8C**), of the Ca^{2+} transients in M2. We conclude there is a progressive engagement of M2 neurons in cocaine mice in distinguishing ALP *vs*. ILP.

DISCUSSION

This study is the first to identify, in real time, the individual and ensemble neuronal engagement of cortical M2 neurons during drug-taking behaviors. In the present study, we analyzed Ca^{2+} transients by three different readouts. The first one was the total Ca^{2+} transients, calculated as the sum of the Ca^{2+} transient amplitude in an assigned time window. The other two were the frequency of Ca^{2+} transients in the corresponding time window and the average amplitude which were calculated by dividing the total Ca^{2+} transients by the frequency. The 15-min time window was used for data analyses in **Fig. 2,** as a general depiction of the Ca^{2+} influx, which was not associated with any individual IVSA event, at the early *vs*. late IVSA daily sessions. When we ran the individual IVSA event-associated Ca^{2+} transient data analyses, the 30-sec time window was used as a basic bin to explore the dynamic changes associated with ALP, ILP, and RNF, with high temporal resolution (**Figs. 3-8, S1-S7**).

When differences in the total Ca^{2+} transients were detected, the frequency and amplitude were also examined to identify the underlying cause of changes in total Ca^{2+} transients. For example, we found that the acute adaptations of Ca^{2+} transients in saline mice were primarily associated with temporary reductions of Ca^{2+} transient frequency in each daily session, whereas the chronic adaptations in cocaine mice were associated with increased frequency and amplitude of Ca^{2+} transients. Second, the IVSA-event based M2 neuronal category was similar when the total Ca^{2+} transients, their frequency or amplitude were used as the Ca^{2+} influx readout before ALP and ILP in both saline and cocaine mice. However, the differences between cocaine *vs*. saline mice in their response to RNF is primarily attributable to the frequency but not the amplitude of Ca^{2+} transients. Third, the

LAN% and the overlap of LANs between ALP/RNFS vs. ILP in cocaine mice are primarily associated with the frequency of Ca^{2+} transients in M2. Thus, the frequency but not the amplitude of the Ca^{2+} transients in M2 neurons is critically involved in the drug taking behaviors and also responded to the RNF.

What do the changes of Ca^{2+} transients mean? It is widely accepted that the changes in neuronal Ca^{2+} transients detected by *in vivo* Ca^{2+} imaging using miniScopes are fundamental processes and a reflection of neuronal activation. They are different from but highly related to action potentials (APs) detected by electrophysiological recordings. Both the Ca^{2+} transient and the AP are triggered by depolarization of the neuronal membrane, although the source and timing of depolarization differ between the two. Both result in changes in membrane potential. However, the nature of these changes and their consequences differ. Neuronal Ca^{2+} transients involve Ca^{2+} influx into the neuron through voltage- or ligand-gated calcium channels. Ca^{2+} influx typically occurs in response to various stimuli, such as neurotransmitter release or membrane depolarization. APs are rapid, transient changes in membrane potential caused by the sequential opening and closing of voltage-gated ion channels, primarily sodium (Na^{+}) and potassium (K^{+}) channels. APs result from a specific threshold level of depolarization being reached, leading to a rapid depolarization followed by repolarization of the membrane potential. As the most pivotal intracellular second messenger, Ca^{2+} influx during Ca^{2+} transients play a crucial role in various cellular processes, including gene expression and intracellular signaling cascades, as well as neurotransmitter release, synaptic plasticity at the axonal and dendrite branches. Ca^{2+} transients do not propagate actively along the neuron, instead, they occur locally in response to specific

stimuli at dendrites, somata, or synaptic terminals. APs are the fundamental means by which neurons not only regulate their own functional level but also transmit electrical signals over long distances. APs propagate actively along the axon of the neuron, facilitated by the regenerative opening of voltage-gated ion channels. This allows for the rapid transmission of signals over long distances. Thus, while both neuronal Ca^{2+} transients and APs involve changes in membrane potential and can be triggered by depolarization, they differ in their underlying mechanisms, functions, and propagation characteristics.

The neuronal Ca^{2+} transients, as a directly indicator of intracellular signaling and modulation of cellular processes, could be directly triggered by APs, but not all APs are associated with a Ca^{2+} transient. For example, the influx of Ca^{2+} during each AP could be lower than the threshold of Ca^{2+} influx to be detected as Ca^{2+} transients, thus there is a minimal number of APs within certain time window to be reached for triggering a Ca^{2+} transient. We call this group of APs corresponding to an individual Ca^{2+} transient as an AP train. It is quantified by the amplitude of Ca^{2+} transients. Two adjacent but distinct Ca^{2+} transients are assumed to be generated by (1) two trains of APs with a long-enough interval and/or (2) a continuous burst of APs interrupted by a refractory period during which no further Ca^{2+} influx occurs as a consequence of Ca^{2+} accumulation intracellularly. Thus, the amplitude and frequency of Ca^{2+} transients are related to APs but not paced exclusively by APs, i.e., there is no precise correspondence between APs and Ca^{2+} transients.

Saline and cocaine IVSA lead to acute vs. chronic adaptation of neuronal activity in M2, respectively: Different from previous traditional neurobiological studies, which either had no longitudinal time window to observe the effects of saline IVSA, or reported no changes in saline group by IVSA procedures, we found that saline mice had a significant behavioral adaptation within the 1-hr daily sessions on both Day 1 and Day 5, i.e., reduction of the # of ALP, ILP and RNF from the first 15 min to the last 15 min of the 1-hr session on both Day 1 and Day 5 (**Fig. 1F-H**). The *in vivo* Ca^{2+} imaging data from saline mice demonstrated that neuronal activity in M2 was also altered in parallel within, but not between daily sessions. For example, we found decreases of the general Ca^{2+} transients from the first to the last 15 min on both Day 1 and Day 5. The LAN% associated with ALP, ILP and RNFs (**Figs. 6A, E, I; 7A**). Thus, the within 1-hr daily session adaptations in saline mice are significant but fully reversible. However, opposite from the observations in saline mice, cocaine mice demonstrated behavioral and neural adaptations are not fully reversible after repeated daily IVSA sessions. The linear increases of inter-ALP-interval in the first 15 min was not observed in the last 15 min due to the equalization of inter-ALP intervals. This persistence of ALPs was maintained throughout the 1-hr IVSA session on Day 5 (**Fig. 1T, U**). Notably, we observed that some of the altered M2 neuronal features, including the general (i.e., IVSA-event non-associated) Ca^{2+} transients (**Fig. 2**), increased Pos% and decreased Neg% after RNF, and reduced LAN% associated with ILP (**Fig. 7B**), at the late stage on Day 1 were well maintained throughout the 1-hr daily session on Day 5 in cocaine mice. We conclude that repeated cocaine IVSA resulted in chronic neuronal adaptations in M2.

From the early to the late stage of IVSA daily sessions on both Day 1 and Day 5, the proportion of three different neuronal clusters based on the relative changes of Ca^{2+} transients (i.e., Pos, NR, and Neg) were consistently maintained before ALP or ILP in both saline and cocaine mice. Lower Pos% and higher Neg% were detected before ALP in cocaine mice, relative to those in saline mice. There were no significant differences of Pos% or Neg% between saline vs. cocaine mice detected before ILP. Thus, the changes observed before ALP cannot be simply attributed to the lever press itself but more related to the associated output (i.e., RNF only initiated after ALP but not ILP). When we looked into the subtypes of neuronal clusters in M2, we identified that consistently higher Neg% before ALP in cocaine mice on both Day 1 and Day 5 should be attributed to the higher Neg_{only}% on Day 1 and higher Neg_{mixed}% on Day 5, respectively. The changes of subtype neuronal proportions from Day 1 to Day 5 was absent before ILP in cocaine mice. Relative to the neurons categorized as Neg_{mixed}, the Neg_{only} neurons are assumed to be better correlated with a consistent reduction of Ca^{2+} influx. Thus, we conclude that synchronized M2 activities seem necessary to initiate the cocaine taking behaviors on Day 1, and a relative lower level of synchronized reduction of Ca^{2+} influx to M2 neurons seems sufficient to initiate the cocaine taking behaviors on Day 5. Our data indicate that the adaptation of M2 neurons by the drug taking experience on early days facilitates the maintenance of persistent cocaine taking behaviors on later days. This real time adaptations observed in M2 may provide a neuronal substrate to explain the transition of drug use to drug mis-use as observed in the laboratory animal model and in clinical human cases.

CONCLUSIONS: M2 neurons are sensitive to and significantly affected by the previous operant behaviors and the history of drug exposure, which in turn sculpt the upcoming operant behaviors and the response to drugs. As critical nodes of the loop, M2 neurons appear to be the governing center in facilitating the establishment of addiction-like behaviors associated with chronic functional changes.

AUTHOR CONTRIBUTION

Experimental design: YC, CG, YYM. Data collection: YC. Data analysis: YC, HF, AK, MAL, CR, DL, SF, CG, YYM. Result discussion: YC, HF, AK, MAL, CR, LT, DL, CG, YYM. Manuscript preparation: YC, FH, AK, MAL, CG, YYM.

FINANCIAL DISCLOSURES

This work was supported by NIH grants (R01AG072897, R21NS108128, and R01AA025784). This work also received support from the Indiana Spinal Cord & Brain Injury Research Fund (Indiana State Department of Health); its contents are solely the responsibility of the providers and do not necessarily represent the official views of the Indiana State Department of Health.

All the authors reported no biomedical financial interests or potential conflicts of interest.

REFERENCES

1. Fact sheeets: Tobacco Detail. World Health Organization. 2022.
2. Orgonization WH. World Health Statistics 2022: Monitoring Health for the Sustainable Development Goals2022.
3. Abuse NIoD. Drug Overdose Death Rates: Trends & Statistics2024.
4. Huang D, Ma YY. Increased Excitability of Layer 2 Cortical Pyramidal Neurons in the Supplementary Motor Cortex Underlies High Cocaine-Seeking Behaviors. Biol Psychiatry. 2023. Epub 20230615. doi: 10.1016/j.biopsych.2023.06.002. PubMed PMID: 37330163.
5. Johanson CE. The evaluation of the abuse liability of drugs. Drug safety. 1990;5 Suppl 1:46-57. PubMed PMID: 2182063.
6. Johanson CE, Balster RL. A summary of the results of a drug self-administration study using substitution procedures in rhesus monkeys. Bulletin on narcotics. 1978;30(3):43-54. PubMed PMID: 36945.
7. Enga RM, Jackson A, Damaj MI, Beardsley PM. Oxycodone physical dependence and its oral self-administration in C57BL/6J mice. European journal of pharmacology. 2016;789:75-80. Epub 2016/07/10. doi: 10.1016/j.ejphar.2016.07.006. PubMed PMID: 27393461; PMCID: PMC5824624.
8. Mayer-Blackwell B, Schlussman SD, Butelman ER, Ho A, Ott J, Kreek MJ, Zhang Y. Self administration of oxycodone by adolescent and adult mice affects striatal neurotransmitter receptor gene expression. Neuroscience. 2014;258:280-91. Epub 2013/11/14. doi: 10.1016/j.neuroscience.2013.10.062. PubMed PMID: 24220688; PMCID: PMC3931009.
9. Zhang Y, Mayer-Blackwell B, Schlussman SD, Randesi M, Butelman ER, Ho A, Ott J, Kreek MJ. Extended access oxycodone self-administration and neurotransmitter receptor gene expression in the dorsal striatum of adult C57BL/6 J mice. Psychopharmacology. 2014;231(7):1277-87. Epub 2013/11/14. doi: 10.1007/s00213-013-3306-3. PubMed PMID: 24221825; PMCID: PMC3954898.
10. Zhang Y, Windisch K, Altschuler J, Rahm S, Butelman ER, Kreek MJ. Adolescent oxycodone self administration alters subsequent oxycodone-induced conditioned place preference and anti-nociceptive effect in C57BL/6J mice in adulthood. Neuropharmacology. 2016;111:314-22. Epub 2016/09/11. doi: 10.1016/j.neuropharm.2016.09.005. PubMed PMID: 27614221; PMCID: PMC5812364.
11. Beacher NJ, Washington KA, Zhang Y, Li Y, Lin DT. GRIN lens applications for studying neurobiology of substance use disorder. Addict Neurosci. 2022;4. Epub 20221124. doi: 10.1016/j.addicn.2022.100049. PubMed PMID: 36531187; PMCID: PMC9757736.
12. Method of the Year 2018: Imaging in freely behaving animals. Nat Methods. 2019;16(1):1. doi: 10.1038/s41592-018-0292-8. PubMed PMID: 30573832.
13. Ghosh KK, Burns LD, Cocker ED, Nimmerjahn A, Ziv Y, Gamal AE, Schnitzer MJ. Miniaturized integration of a fluorescence microscope. Nat Methods. 2011;8(10):871-8. Epub 20110911. doi: 10.1038/nmeth.1694. PubMed PMID: 21909102; PMCID: PMC3810311.
14. Cai DJ, Aharoni D, Shuman T, Shobe J, Biane J, Song W, Wei B, Veshkini M, La-Vu M, Lou J, Flores SE, Kim I, Sano Y, Zhou M, Baumgaertel K, Lavi A, Kamata M,

Tuszynski M, Mayford M, Golshani P, Silva AJ. A shared neural ensemble links distinct contextual memories encoded close in time. Nature. 2016;534(7605):115-8. Epub 20160523. doi: 10.1038/nature17955. PubMed PMID: 27251287; PMCID: PMC5063500.
15. Marchette RCN, Tunstall BJ, Vendruscolo LF, Moussawi K. Operant Vapor Self-administration in Mice. Bio Protoc. 2021;11(10):e4023. Epub 20210520. doi: 10.21769/BioProtoc.4023. PubMed PMID: 34150930; PMCID: PMC8187126.
16. Vollmer KM, Green LM, Grant RI, Winston KT, Doncheck EM, Bowen CW, Paniccia JE, Clarke RE, Tiller A, Siegler PN, Bordieanu B, Siemsen BM, Denton AR, Westphal AM, Jhou TC, Rinker JA, McGinty JF, Scofield MD, Otis JM. An opioid-gated thalamoaccumbal circuit for the suppression of reward seeking in mice. Nat Commun. 2022;13(1):6865. Epub 20221111. doi: 10.1038/s41467-022-34517-w. PubMed PMID: 36369508; PMCID: PMC9652456.
17. Sun Y, Giocomo LM. Neural circuit dynamics of drug-context associative learning in the mouse hippocampus. Nat Commun. 2022;13(1):6721. Epub 20221107. doi: 10.1038/s41467-022-34114-x. PubMed PMID: 36344498; PMCID: PMC9640587.
18. Colucci SV, Perrino PJ, Shram M, Bartlett C, Wang Y, Harris SC. Abuse potential of intravenous oxycodone/naloxone solution in nondependent recreational drug users. Clin Drug Investig. 2014;34(6):421-9. Epub 2014/04/24. doi: 10.1007/s40261-014-0192-3. PubMed PMID: 24756361; PMCID: PMC4026623.
19. Ma YY, Cepeda C, Chatta P, Franklin L, Evans CJ, Levine MS. Regional and cell-type-specific effects of DAMGO on striatal D1 and D2 dopamine receptor-expressing medium-sized spiny neurons. ASN neuro. 2012;4(2). Epub 2012/01/26. doi: 10.1042/an20110063. PubMed PMID: 22273000; PMCID: PMC3297119.
20. Ma YY, Lee BR, Wang X, Guo C, Liu L, Cui R, Lan Y, Balcita-Pedicino JJ, Wolf ME, Sesack SR, Shaham Y, Schluter OM, Huang YH, Dong Y. Bidirectional modulation of incubation of cocaine craving by silent synapse-based remodeling of prefrontal cortex to accumbens projections. Neuron. 2014;83(6):1453-67. Epub 2014/09/10. doi: 10.1016/j.neuron.2014.08.023. PubMed PMID: 25199705; PMCID: PMC4295617.
21. Ma YY, Wang X, Huang Y, Marie H, Nestler EJ, Schluter OM, Dong Y. Re-silencing of silent synapses unmasks anti-relapse effects of environmental enrichment. Proceedings of the National Academy of Sciences of the United States of America. 2016;113(18):5089-94. Epub 2016/04/20. doi: 10.1073/pnas.1524739113. PubMed PMID: 27091967; PMCID: PMC4983865.
22. Guo C, Wen D, Zhang Y, Mustaklem R, Mustaklem B, Zhou M, Ma T, Ma YY. Amyloid-beta oligomers in the nucleus accumbens decrease motivation via insertion of calcium-permeable AMPA receptors. Mol Psychiatry. 2022;27(4):2146-57. Epub 20220202. doi: 10.1038/s41380-022-01459-0. PubMed PMID: 35105968; PMCID: PMC9133055.
23. Huang D, Ma YY. Increased Excitability of Layer 2 Cortical Pyramidal Neurons in the Supplementary Motor Cortex Underlies High Cocaine-Seeking Behaviors. Biol Psychiatry. 2023;94(11):875-87. Epub 20230615. doi: 10.1016/j.biopsych.2023.06.002. PubMed PMID: 37330163; PMCID: PMC10721734.
24. Shan L, Galaj E, Ma YY. Nucleus accumbens shell small conductance potassium channels underlie adolescent ethanol exposure-induced anxiety. Neuropsychopharmacology : official publication of the American College of

Neuropsychopharmacology. 2019. Epub 2019/05/17. doi: 10.1038/s41386-019-0415-7. PubMed PMID: 31096263.
25. Dong Z, Mau W, Feng Y, Pennington Z, Chen L, Zaki Y, Rajan K, Shuman T, Aharoni D, Cai DJ. Minian: An open-source miniscope analysis pipeline. bioRxiv. 2021. doi: https://doi.org/10.1101/2021.05.03.442492.

FIGURE LEGENDS

Figure 1. Cocaine taking behaviors.

A, Experimental timeline

B, No differences were observed in the total distance traveled during the 5-min open field test before the IVSA procedure between mice assigned to saline *vs*. cocaine treatment (t_{16}=0.1, p=0.95).

C, Individual mouse values (small circles) and summarized data (large circles) showing no differences between ALP *vs*. ILP during the 5 daily IVSA sessions in saline mice (ALP/ILP × IVSA day interaction $F_{4,28}$=2.8, p=0.04; ALP/ILP $F_{1,7}$=0.4, p=0.53; and IVSA day $F_{4,28}$=0.8, p=0.53).

D, Individual mouse values (small circles) and summarized data (large circles) showing significantly higher ALP, relative to ILP, during the 5 daily IVSA sessions in cocaine mice (ALP/ILP $F_{1,9}$=55.6, p<0.01, in spite of ALP/ILP × IVSA day interaction $F_{4,36}$=0.7, p=0.60; and IVSA day $F_{4,36}$=2.0, p=0.11).

E, Individual mouse values (small circles) and summarized data (large circles) showing a significantly higher RNF number in cocaine mice, relative to saline mice, during the 5 daily IVSA sessions (saline/cocaine × IVSA day interaction $F_{4,64}$=3.1, p=0.02; saline/cocaine $F_{1,16}$=29.7, p<0.01; and IVSA day $F_{4,64}$=1.9, p=0.13).

F-H, Individual mouse values (small circles) and summarized data (large circles) from saline mice showing gradual decreases in the numbers of ALP (**F**, 15-min slot $F_{2,14}$=8.1, p<0.01, despite of IVSA day × 15-min slot interaction $F_{2,14}$=1.6, p=0.24, IVSA day $F_{1,7}$<0.1, p=0.82), ILP (**G**, 15-min slot $F_{2,14}$=10.9, p<0.01, despite of IVSA day × 15-min slot interaction $F_{2,13}$=0.9, p=0.41, IVSA day $F_{1,7}$=0.7, p=0.44) and

RNF (**H**, 15-min slot $F_{2,14}$=10.7, p<0.01, despite of IVSA day × 15-min slot interaction $F_{1,10}$=0.9, p=0.40, IVSA day $F_{1,7}$=0.9, p=0.37) during the 1-hr IVSA sessions on both Day 1 and Day 5.

I-K, Individual mouse values (small circles) and summarized data (large circles) from cocaine mice showing higher number of ALP (**I**, IVSA day $F_{1,9}$=5.3, p=0.047, despite of IVSA day × 15-min slot interaction $F_{2,17}$=1.3, p=0.34, 15-min slot $F_{2,18}$=0.6, p=0.54) and RNF (**K**, IVSA day $F_{1,9}$=5.5, p=0.04, despite of IVSA day × 15-min slot interaction $F_{3,27}$=0.5, p=0.69, 15-min slot $F_{3,27}$=0.2, p=0.90), but not ILP (**J**, IVSA day × 15-min slot interaction $F_{2,22}$=1.0, p=0.39, IVSA day $F_{1,9}$=1.7, p=0.22, 15-min slot $F_{2,16}$=1.5, p=0.24), at the early time of the 1-hr IVSA sessions on Day 5, relative to that on Day 1.

L-Q, Summarized data (**L-N**) and the fitting curves (**O-Q** by non-linear curve fitting in Prism 10, GraphPad) showing the significant interactions of three factors (i.e., saline/cocaine denoted “S/C”, IVSA days denoted “D”, and the minute during the 1-hr IVSA session denoted “min”) on ALP (**L**, S/C × D × min interaction $F_{119,1904}$=1.5, p<0.01; S/C × D interaction $F_{1,16}$=2.1, p=0.16; S/C × min interaction $F_{119,1904}$=2.8, p<0.01; D × min interaction $F_{119,1904}$=6.5, p<0.01; S/C $F_{1,16}$=13.8, p<0.01; D $F_{1,16}$=34.9, p<0.01; min $F_{119,1904}$=224.5, p<0.01) and RNF (**M**, S/C × D × min interaction $F_{119,1904}$=2.2, p<0.01; S/C × D interaction $F_{1,16}$=5.3, p=0.03; S/C × min interaction $F_{119,1904}$=3.0, p<0.01; D × min interaction $F_{119,1904}$=9.6, p<0.01; S/C $F_{1,16}$=15.8, p<0.01; D $F_{1,16}$=44.1, p<0.01; min $F_{119,1904}$=297.0, p<0.01), but not ILP (**N**, S/C × D × min interaction $F_{119,1904}$=0.9, p=0.65; S/C × D interaction $F_{1,16}$<0.01, p=0.93; S/C × min interaction $F_{119,1904}$=1.5, p<0.01; D × min interaction

$F_{119,1904}$=4.0, p<0.01; S/C $F_{1,16}$=2.3, p=0.15; D $F_{1,16}$=2.7, p=0.12; min $F_{119,1904}$=82.3, p<0.01).

R-U, Scatter plots of the inter-ALP interval (y axis, in which 1000 sec was the max interval to the cutoff interval included) during the first (left in each panel) or the last (right in each panel) 15 min in the 1-hr IVSA training (x axis), together with the lines obtained by simply linear regression. In saline mice, significant non-zero linear regression was detected in the first 15 min (left panel in **R**, y=24x − 25, $F_{1,25}$=9.3, p<0.01; r=0.52, p<0.01) but not the last 15 min (right panel in **R**, y=11x − 150, $F_{1,4}$=0.1, p=0.75; r=0.17, p=0.75) during the 1-hr IVSA session on Day 1, whereas neither first 15 min (left panel in **S**, y=3x + 35, $F_{1,47}$=1.0, p=0.32; r=0.15, p=0.32) nor the last 15 min (right panel in **S**, no data points available in this time window) showed any non-zero linear correlations on Day 5 of the 5-day saline IVSA sessions. In cocaine mice, significant non-zero linear regression was detected in the first 15 min but not the last 15 min during the 1-hr IVSA session on both Day 1 (left panel in **T** for the first 15 min, y=21x − 13, $F_{1,39}$=13.7, p<0.01; r=0.51, p<0.01; right panel in **T** for the last 15 min, y= −6x − 484, $F_{1,59}$=1.5, p=0.22; r= −0.16, p=0.22) and Day 5 (left panel in **U** for the first 15 min, y=9x + 37, $F_{1,68}$=9.7, p<0.01; r=0.35, p<0.01; right panel in **U** for the last 15 min, y=−2x + 209, $F_{1,57}$=0.1, p=0.74; r=−0.04, p=0.74) of the 5-day cocaine IVSA sessions.

Data were analyzed by unpaired Student's t test (**B**), two-way ANOVA with repeated measures on (a) Days and ALP/ILP (**C, D**), (b) Days (**E**) or (c) Day1/5 and different 15-min slots (**F-K**), three-way ANOVA with repeated measures on D and min (**L-**

N), and simply linear regression and Pearson correlations (**R-U**). n=8 for saline mice, and n=10 for cocaine mice.

Figure 2. **Ca^{2+} transients in M2 neurons in the first *vs*. last 15 min on Day 1 and Day 5 of IVSA.**

A, Representative images of GCaMP8f in M2 neurons, primarily the pyramidal projection neurons as demonstrated in the lower right panel.

B, Images of maximum projections of *in vivo* Ca^{2+} images from a representative mouse

C-H, Scattered plots showing the total Ca^{2+} transients (**C**, **D**), and their frequency (**E**, **F**) and amplitude (**G**, **H**) in all the Ca^{2+} *in vivo* recording-captured M2 neurons in the first (open circles) and the last (solid circles) 15-min on the first and the last IVSA days in saline (**C**, **E**, **G**) and cocaine (**D**, **F**, **H**) mice.

I-K, Violin plots demonstrating the density of detected M2 neurons at different levels of total Ca^{2+} transients (**I**), and their frequency (**J**) and amplitude (**K**) in the first (open plot) and the last (solid plot) 15-min on the first and the last IVSA days in saline (in grayish) and cocaine (in reddish) mice. There are three dashed lines to split each violin plot at the quartile positions.

L-N, Total Ca^{2+} transient (**L**), and their frequency (**M**) and amplitude (**N**) for each animal in the first (open plot) and the last (solid plot) 15-min on the first and the last IVSA days in saline (in grayish) and cocaine (in reddish) mice.

The # of neurons are provided in **C,D**. Data from each neuron in **C-K** or from each animal in **L-N** were analyzed by three-way ANOVA, followed by Bonferroni's post hoc test as shown in **Table S1** (**C-K**) and **S2** (**L-N**). In **L-N**, *, $p<0.05$; **, $p<0.01$.

Figure 3. **Ca^{2+} transients in M2 neurons during 3 min before ALP in saline vs. cocaine mice.**

A, **B**, Representative Ca^{2+} transient traces within 3 min before ALP in the first (left in each pair of the trace columns) and the last (right in each pair of the trace columns) 15 min during Day 1 and Day 5 IVSA sessions in saline (**A**) and cocaine (**B**) mice.

C, D, Heat maps of ΔZ scores of neuronal total Ca^{2+} transients in detected M2 neurons displayed by rows of six 30-sec blocks within 3 min before ALP in the first (left in each pair of the trace columns) and the last (right in each pair of the trace columns) 15 min during Day 1 and Day 5 IVSA sessions in saline (**C**) and cocaine (**D**) mice.

E-H, Total Ca^{2+} transient ΔZ based-classification of **each** 30-sec block of M2 neurons within 3 min before ALP in the first (left in each pair of the trace columns) *vs*. the last (right in each pair of the trace columns) 15 min during Day 1 and Day 5 IVSA sessions in saline (**E**) and cocaine (**G**) mice. The proportions of M2 neurons in each category in a 15-min session are summarized in **F** for saline mice and **H** for cocaine mice.

I, **J**, Summarized data showing the percentage of three ALP & total Ca^{2+} transient -based categories of M2 neurons in saline (**I**) and cocaine (**J**) mice. Both saline (**I**,

neuron type × IVSA training session interaction $F_{6,40}$=0.4, p=0.86; neuron type $F_{1,20}$=103.2, p<0.01; and IVSA training session $F_{3,20}$=0.0, p>0.99) and cocaine (**J**, neuron type × IVSA training session interaction $F_{6,66}$=0.2, p=0.98; neuron type $F_{1,35}$=238.0, p<0.01; and IVSA training session $F_{3,33}$=0.9, p=0.48) mice demonstrated different proportions among three neuronal types.

K-M, Summarized data showing smaller proportions of ALP & total Ca^{2+} transient -categorized Pos neurons (**K**, saline/cocaine × IVSA training session interaction $F_{3,53}$=0.1, p=0.93; saline/cocaine $F_{1,53}$=21.0, p<0.01; and IVSA training session $F_{3,53}$=0.5, p=0.69), similar proportions of ALP-categorized NR neurons (**L**, saline/cocaine × IVSA training session interaction $F_{3,53}$=0.1, p=0.98; saline/cocaine $F_{1,53}$=0.2, p=0.67; and IVSA training session $F_{3,53}$=0.9, p=0.46), and larger proportions of ALP-categorized Neg neurons (**M**, saline/cocaine × IVSA training session interaction $F_{3,53}$=0.2, p=0.93; saline/cocaine $F_{1,53}$=20.0, p<0.01; and IVSA training session $F_{3,53}$=0.6, p=0.61) in cocaine mice, relative to that in saline mice.

N, **O**, Summarized data showing training session-associated differences in the proportions of ALP & total Ca^{2+} transient -categorized Pos_{pure} neurons (**N**, saline/cocaine × IVSA training session interaction $F_{3,53}$=11.7, p<0.01; saline/cocaine $F_{1,53}$=1.7, p=0.19; and IVSA training session $F_{3,53}$=13.2, p<0.01), and ALP-categorized Pos_{mixed} neurons (**O**, saline/cocaine × IVSA training session interaction $F_{3,53}$=1.3, p=0.29; saline/cocaine $F_{1,53}$=24.8, p<0.01; and IVSA training session $F_{3,53}$=1.1, p=0.36)between saline *vs*. cocaine mice.

P, **Q**, Summarized data showing training session-associated differences in the proportions of ALP & total Ca^{2+} transient -categorized Neg_{pure} neurons (**P**, saline/cocaine × IVSA training session interaction $F_{3,53}$=7.0, p<0.01; saline/cocaine $F_{1,53}$=8.5, p<0.01; and IVSA training session $F_{3,53}$=8.5, p<0.01), and ALP-categorized Neg_{mixed} neurons (**Q**, saline/cocaine × IVSA training session interaction $F_{3,53}$=4.5, p=0.01; saline/cocaine $F_{1,53}$=18.0, p<0.01; and IVSA training session $F_{3,53}$=8.9, p<0.01) between saline *vs*. cocaine mice.

Data were analyzed by two-way ANOVA with repeated measures on neuron types and IVSA sessions (**I**, **J**), on IVSA sessions (**K-Q**), followed by Bonferroni *post hoc* test. Between different IVSA sessions, *, p<0.05; **, p<0.01. Within saline or within cocaine, #, p<0.05; ##, 0.01.

Figure 4. **Ca^{2+} transients in M2 neurons during 3 min before ILP in saline vs. cocaine mice.**

A, **B**, Representative Ca^{2+} transient traces within 3 min before ILP in the first (left in each pair of the trace columns) and the last (right in each pair of the trace columns) 15 min during Day 1 and Day 5 IVSA sessions in saline (**A**) and cocaine (**B**) mice.

C, D, Heat maps of ΔZ scores of neuronal total Ca^{2+} transients in detected M2 neurons displayed by rows of six 30-sec blocks within 3 min before ILP in the first (left in each pair of the trace columns) and the last (right in each pair of the trace columns) 15 min during Day 1 and Day 5 IVSA sessions in saline (**C**) and cocaine (**D**) mice.

E-H, Total Ca^{2+} transient ΔZ-based classification of **each** 30-sec block of M2 neurons within 3 min before ILP in the first (left in each pair of the trace columns) *vs*. the last (right in each pair of the trace columns) 15 min during Day 1 and Day 5 IVSA sessions in saline (**E**) and cocaine (**G**) mice. The proportions of M2 neurons in each category in a 15-min session is summarized in **F** for saline mice and **H** for cocaine mice.

I, **J**, Summarized data showing the percentage of three ILP & total Ca^{2+} transient -based categories of M2 neurons in saline (**I**) and cocaine (**J**) mice. Both saline (**I**, neuron type × IVSA training session interaction $F_{6,40}<0.1$, $p>0.99$; neuron type $F_{1,20}=71.8$, $p<0.01$; and IVSA training session $F_{3,20}=155.4$, $p<0.01$) and cocaine (**J**, neuron type × IVSA training session interaction $F_{6,66}=0.2$, $p=0.98$; neuron type $F_{1,33}=222.0$, $p<0.01$; and IVSA training session $F_{3,33}=0.5$, $p=0.69$) mice demonstrated different proportions among three neuronal types.

K-M, Summarized data showing similar proportions of ILP & total Ca^{2+} transient -categorized Pos neurons (**K**, saline/cocaine × IVSA training session interaction $F_{3,53}=0.2$, $p=0.87$; saline/cocaine $F_{1,53}=3.1$, $p=0.08$; and IVSA training session $F_{3,53}=0.4$, $p=0.77$), ILP-categorized NR neurons (**L**, saline/cocaine × IVSA training session interaction $F_{3,53}=1.2$, $p=0.31$; saline/cocaine $F_{1,53}=3.2$, $p=0.08$; and IVSA training session $F_{3,53}=1.6$, $p=0.19$), and ILP-categorized Neg neurons (**M**, saline/cocaine × IVSA training session interaction $F_{3,53}=0.2$, $p=0.86$; saline/cocaine $F_{1,53}=3.7$, $p=0.06$; and IVSA training session $F_{3,53}=0.3$, $p=0.82$) between saline *vs*. cocaine mice.

N, **O**, Summarized data showing significant differences in the proportions of ILP & total Ca^{2+} transient -categorized Pos_{pure} neurons (**N**, saline/cocaine × IVSA training session interaction $F_{3,53}$=3.4, p=0.03; saline/cocaine $F_{1,53}$=6.0, p=0.02; and IVSA training session $F_{3,53}$=16.0, p<0.01), and ILP-categorized Pos_{mixed} neurons (**O**, saline/cocaine × IVSA training session interaction $F_{3,53}$=0.5, p=0.68; saline/cocaine $F_{1,53}$=9.3, p<0.01; and IVSA training session $F_{3,53}$=2.4, p=0.08) between saline *vs*. cocaine mice.

P, **Q**, Summarized data showing no detectable differences in the proportions of ILP & total Ca^{2+} transient-categorized Neg_{pure} neurons (**P**, saline/cocaine × IVSA training session interaction $F_{3,53}$=2.0, p=0.12; saline/cocaine $F_{1,53}$=2.7, p=0.11; and IVSA training session $F_{3,53}$=0.2, p=0.93), or ILP-categorized Neg_{mixed} neurons (**Q**, saline/cocaine × IVSA training session interaction $F_{3,53}$=0.1, p=0.97; saline/cocaine $F_{1,53}$=3.6, p=0.06; and IVSA training session $F_{3,53}$=0.5, p=0.71) between saline *vs*. cocaine mice.

Data were analyzed by two-way ANOVA with repeated measures on neuron types and IVSA sessions (**I**, **J**), on IVSA sessions (**K-Q**), followed by Bonferroni *post hoc* test. Between different IVSA sessions, *, p<0.05; **, p<0.01. Within saline or within cocaine, #, p<0.05; ##, 0.01.

Figure 5. **Ca^{2+} transients in M2 neurons with 3 min after RNF in saline vs. cocaine mice.**

A, **B**, Representative Ca^{2+} transient traces within 3 min after RNF in the first (left in each pair of the trace columns) and the last (right in each pair of the trace columns) 15 min during Day 1 and Day 5 IVSA sessions in saline (**A**) and cocaine (**B**) mice.

C, D, Heat maps of ΔZ scores of neuronal total Ca^{2+} transients in detected M2 neurons displayed by rows of six 30-sec blocks within 3 min after RNF in the first (left in each pair of the trace columns) and the last (right in each pair of the trace columns) 15 min during Day 1 and Day 5 IVSA sessions in saline (**C**) and cocaine (**D**) mice.

E-H, Total Ca^{2+} transient ΔZ-based classification of **each** 30-sec block of M2 neuron within 3 min after RNF in the first (left in each pair of the trace columns) *vs*. the last (right in each pair of the trace columns) 15 min during Day 1 and Day 5 IVSA sessions in saline (**E**) and cocaine (**G**) mice. The proportions of M2 neurons in each category in a 15-min session is summarized in **F** for saline mice and **H** for cocaine mice.

I, **J**, Summarized data showing the percentage of three RNF & total Ca^{2+} transient -based categories of M2 neurons in saline (**I**) and cocaine (**J**) mice. Both saline (**I**, neuron type × IVSA training session interaction $F_{6,40}=0.2$, $p=0.98$; neuron type $F_{1,23}=59.2$, $p<0.01$; and IVSA training session $F_{3,20}<0.1$, $p>0.99$) and cocaine (**J**, neuron type × IVSA training session interaction $F_{6,66}=5.7$, $p<0.01$; neuron type $F_{1,39}=149.3$, $p<0.01$; and IVSA training session $F_{3,33}=128.9$, $p<0.01$) mice demonstrated different proportions among three neuronal types.

K-M, Summarized data showing lower proportions of RNF & total Ca^{2+} transient -categorized Pos neurons (**K**, saline/cocaine × IVSA training session interaction

$F_{3,53}$=1.1, p=0.36; saline/cocaine $F_{1,53}$=8.4, p=0.01; and IVSA training session $F_{3,53}$=2.8, p=0.049), similar proportions of RNF & total Ca^{2+} transient-categorized NR neurons (**L**, saline/cocaine × IVSA training session interaction $F_{3,53}$=0.8, p=0.49; saline/cocaine $F_{1,53}$=3.3, p=0.08; and IVSA training session $F_{3,53}$=0.8, p=0.47), and higher proportions of RNF & total Ca^{2+} transient -categorized Neg neurons (**M**, saline/cocaine × IVSA training session interaction $F_{3,53}$=1.5, p=0.22; saline/cocaine $F_{1,53}$=14.7, p<0.01; and IVSA training session $F_{3,53}$=3.2, p=0.03) in cocaine mice, relative to that in saline mice.

N, **O**, Summarized data showing training session-associated differences in the proportions of RNF & total Ca^{2+} transient-categorized Pos_{pure} neurons (**N**, saline/cocaine × IVSA training session interaction $F_{3,53}$=1.3, p=0.29; saline/cocaine $F_{1,53}$=4.4, p=0.04; and IVSA training session $F_{3,53}$=1.6, p=0.21), and RNF-categorized Pos_{mixed} neurons (**O**, saline/cocaine × IVSA training session interaction $F_{3,53}$=1.0, p=0.42; saline/cocaine $F_{1,53}$=13.8, p<0.01; and IVSA training session $F_{3,53}$=1.8, p=0.15) between saline *vs*. cocaine mice.

P, **Q**, Summarized data showing training session-associated differences in the proportions of RNF & total Ca^{2+} transient -categorized Neg_{pure} neurons (**P**, saline/cocaine × IVSA training session interaction $F_{3,53}$=7.9, p<0.01; saline/cocaine $F_{1,53}$=28.1, p<0.01; and IVSA training session $F_{3,53}$=12.6, p<0.01), and RNF-categorized Neg_{mixed} neurons (**Q**, saline/cocaine × IVSA training session interaction $F_{3,53}$=0.2, p=0.89; saline/cocaine $F_{1,53}$=4.4, p=0.04; and IVSA training session $F_{3,53}$=1.8, p=0.161) between saline *vs*. cocaine mice.

Data were analyzed by two-way ANOVA with repeated measures on neuron types and IVSA sessions (**I**, **J**), on IVSA sessions (**K-Q**), followed by Bonferroni's *post hoc* test. Between different IVSA sessions, *, $p<0.05$; **, $p<0.01$. Within saline or within cocaine, #, $p<0.05$; ##, 0.01.

Figure 6. Non-cumulative *vs*. cumulative effects of cocaine-associated events on Ca2+ transients in M2 neurons.

A-D, % of linearly associated neurons (LANs) analyzed with the non-cumulative (nonCML) and cumulative (CML) ALP #s on Ca^{2+} transients detected in M2 neurons. ACC-LANs in M2 were detected with a higher number in both saline (**A**, nonCML/CML × IVSA training session interaction $F_{2,13}=3.9$, $p=0.047$; nonCML/CML $F_{1,7}=44.8$, $p<0.01$; and IVSA training session $F_{3,19}=4.0$, $p=0.03$) and cocaine (**B**, nonCML/CML × IVSA training session interaction $F_{2,17}=2.3$, $p=0.13$; nonCML/CML $F_{1,9}=21.0$, $p<0.01$; and IVSA training session $F_{3,23}=0.5$, $p=0.67$) mice. The % of nonACC LANs (**C**, saline/cocaine × IVSA training session interaction $F_{3,48}=1.6$, $p=0.20$; saline/cocaine $F_{1,16}=16.2$, $p<0.01$; and IVSA training session $F_{3,48}=0.9$, $p=0.44$) and the ACC LANs (**D**, saline/cocaine × IVSA training session interaction $F_{3,48}=0.1$, $p=0.93$; saline/cocaine $F_{1,16}=6.5$, $p=0.02$; and IVSA training session $F_{3,48}=4.1$, $p=0.01$) were higher in cocaine mice, relative to that in saline mice.

E-H, % of LANs analyzed with nonACC and ACC ILP #s on Ca^{2+} transients detected in M2 neurons. ACC-LANs in M2 were detected with a higher number in both saline (**E**, nonCML/CML × IVSA training session interaction $F_{2,15}=2.2$, $p=0.14$;

nonCML/CML $F_{1,7}$=19.4, p<0.01; and IVSA training session $F_{2,17}$=6.3, p=0.01) and cocaine (**F**, nonCML/CML × IVSA training session interaction $F_{2,18}$=6.3, p=0.01; nonCML/CML $F_{1,9}$=6.7, p=0.03; and IVSA training session $F_{2,15}$=2.0, p=0.17) mice. The % of nonACC LANs (**G**, saline/cocaine × IVSA training session interaction $F_{3,48}$=2.1, p=0.12; saline/cocaine $F_{1,16}$=0.5, p=0.48; and IVSA training session $F_{3,48}$=1.3, p=0.27) and the ACC LANs (**H**, saline/cocaine × IVSA training session interaction $F_{3,48}$=2.2, p=0.10; saline/cocaine $F_{1,16}$=1.7, p=0.21; and IVSA training session $F_{3,48}$=7.5, p<0.01).

I-L, % of LANs analyzed with the non-cumulative (nonCML) and cumulative (CML) RNF #s on Ca^{2+} transients detected in M2 neurons. ACC-LANs in M2 were detected with a higher number in both saline (**I**, nonCML/CML × IVSA training session interaction $F_{2,16}$=2.1, p=0.15; nonCML/CML $F_{1,7}$=40.1, p<0.01; and IVSA training session $F_{2,13}$=3.9, p=0.046) and cocaine (**J**, nonCML/CML × IVSA training session interaction $F_{2,19}$=1.1, p=0.36; nonCML/CML $F_{1,9}$=20.2, p<0.01; and IVSA training session $F_{2,16}$=2.7, p=0.10) mice. The % of nonACC LANs (**K**, saline/cocaine × IVSA training session interaction $F_{3,48}$=1.1, p=0.34; saline/cocaine $F_{1,16}$=8.0, p=0.01; and IVSA training session $F_{3,48}$=1.6, p=0.20) and the ACC LANs (**L**, saline/cocaine × IVSA training session interaction $F_{3,48}$=0.1, p=0.95; saline/cocaine $F_{1,16}$=5.4, p=0.03; and IVSA training session $F_{3,48}$=4.3, p=0.01) were higher in cocaine mice, relative to that in saline mice.

Data were analyzed by two-way ANOVA with repeated measures, followed by Bonferroni's post-test. *p<0.05, **p<0.01, marked in green as comparisons

between nonACC *vs*. ACC, blue as comparisons between different IVSA sessions, or purple as comparations between saline *vs*. cocaine.

Figure. 7 % of positive vs. negative LANs in M2 during saline or cocaine taking.

A, **B**, % of the positive (in sections with no filling) *vs*. negative (in sections with shadow) LANs identified by linear regression analyses of cumulative # of *in vivo* events, including ALP (left column), ILP (middle column) and RNF (right column), respectively, with the Ca^{2+} transient (i.e., the sum of the amplitude) in each 30-sec block from individual neurons in M2 during the first or the last 15 min on Day 1 or Day 5 of saline (**A**) or cocaine (**B**) IVSA.

C, D, Figure legends demonstrating how to calculate (1) the % of LANs, which determines the size of each circle (**C**), and (2) the % of Pos LANs or % of Neg LANs which determines the ratio of two sections in each circle (**D**).

Figure 8. Distribution of IVSA event-associated LANs in M2.

A-C, Proportional Venn diagrams showing the distribution of M2 neurons with linear association to one or multiple *in vivo* events (i.e., ALP, ILP, or RNF) during the first and the last 15 min of the one-hour saline (upper panels) and cocaine (lower panels) IVSA procedures on Day 1 and Day 5. Ca^{2+} transient quantification was made by the Ca^{2+} transient (i.e., the sum of the amplitude) (**A**), the frequency of the Ca^{2+} transients (**B**), and the amplitude of the Ca^{2+} transients (i.e., the average amplitude) (**C**) in each 30-sec block, which was analyzed by linear regression with the cumulative # of *in vivo* events (i.e., ALP, ILP, RNF) in the corresponding 30-sec block in each 15-min session from individual M2 neurons.

D, E, Figure legends showing the color codes for different IVSA events and their overlaps (**D**) and the scale of circle size representing the % of LANs (**E**).

Figure S1. **The frequency of Ca^{2+} transients in M2 neurons during 3 min before ALP in saline *vs*. cocaine mice.**

A, **B**, Heat maps of ΔZ scores of neuronal Ca^{2+} transient frequency in detected M2 neurons displayed by rows of six 30-sec blocks within 3 min before ALP in the first (left in each pair of the trace columns) and the last (right in each pair of the trace columns) 15 min during Day 1 and Day 5 IVSA sessions in saline (**A**) and cocaine (**B**) mice.

C-F, Ca^{2+} transient frequency ΔZ based-classification of each 30-sec block of M2 neurons within 3 min before ALP in the first *vs*. the last 15 min during Day 1 and Day 5 IVSA sessions in saline (**C**) and cocaine (**E**) mice. The proportions of M2 neurons in each category in a 15-min session are summarized in **D** for saline mice and **F** for cocaine mice.

Figure S2. **The amplitude of Ca^{2+} transients in M2 neurons during 3 min before ALP in saline *vs*. cocaine mice.**

A, **B**, Heat maps of ΔZ scores of neuronal Ca^{2+} transient amplitude in detected M2 neurons displayed by rows of six 30-sec blocks within 3 min before ALP in the first (left in each pair of the trace columns) and the last (right in each pair of the trace columns) 15 min during Day 1 and Day 5 IVSA sessions in saline (**A**) and cocaine (**B**) mice.

C-F, Ca^{2+} transient amplitude ΔZ based-classification of each 30-sec block of M2 neurons within 3 min before ALP in the first *vs*. the last 15 min during Day 1 and Day 5 IVSA sessions in saline (**C**) and cocaine (**E**) mice. The proportions of M2 neurons in each category in a 15-min session are summarized in **D** for saline mice and **F** for cocaine mice.

Figure S3. **The frequency of Ca^{2+} transients in M2 neurons during 3 min before ILP in saline *vs*. cocaine mice.**

A, **B**, Heat maps of ΔZ scores of neuronal Ca^{2+} transient frequency in detected M2 neurons displayed by rows of six 30-sec blocks within 3 min before ILP in the first (left in each pair of the trace columns) and the last (right in each pair of the trace columns) 15 min during Day 1 and Day 5 IVSA sessions in saline (**A**) and cocaine (**B**) mice.

C-F, Ca^{2+} transient frequency ΔZ based-classification of each 30-sec block of M2 neurons within 3 min before ILP in the first *vs*. the last 15 min during Day 1 and Day 5 IVSA sessions in saline (**C**) and cocaine (**E**) mice. The proportions of M2 neurons in each category in a 15-min session are summarized in **D** for saline mice and **F** for cocaine mice.

Figure S4. **The amplitude of Ca^{2+} transients in M2 neurons during 3 min before ILP in saline *vs*. cocaine mice.**

A, **B**, Heat maps of ΔZ scores of neuronal Ca^{2+} transient amplitude in detected M2 neurons displayed by rows of six 30-sec blocks within 3 min before ILP in the first (left in each pair of the trace columns) and the last (right in each pair of the trace

columns) 15 min during Day 1 and Day 5 IVSA sessions in saline (**A**) and cocaine (**B**) mice.

C-F, Ca^{2+} transient amplitude ΔZ based-classification of each 30-sec block of M2 neurons within 3 min before ILP in the first *vs*. the last 15 min during Day 1 and Day 5 IVSA sessions in saline (**C**) and cocaine (**E**) mice. The proportions of M2 neurons in each category in a 15-min session are summarized in **D** for saline mice and **F** for cocaine mice.

Figure S5. **The frequency of Ca^{2+} transients in M2 neurons during 3 min after RNF in saline *vs*. cocaine mice.**

A, **B**, Heat maps of ΔZ scores of neuronal Ca^{2+} transient frequency in detected M2 neurons displayed by rows of six 30-sec blocks within 3 min after RNF in the first (left in each pair of the trace columns) and the last (right in each pair of the trace columns) 15 min during Day 1 and Day 5 IVSA sessions in saline (**A**) and cocaine (**B**) mice.

C-F, Ca^{2+} transient frequency ΔZ based-classification of each 30-sec block of M2 neurons within 3 min after RNF in the first *vs*. the last 15 min during Day 1 and Day 5 IVSA sessions in saline (**C**) and cocaine (**E**) mice. The proportions of M2 neurons in each category in a 15-min session are summarized in **D** for saline mice and **F** for cocaine mice.

Figure S6. **The amplitude of Ca^{2+} transients in M2 neurons during 3 min after RNF in saline *vs*. cocaine mice.**

A, **B**, Heat maps of ΔZ scores of neuronal Ca^{2+} transient amplitude in detected M2 neurons displayed by rows of six 30-sec blocks within 3 min after RNF in the first (left in each pair of the trace columns) and the last (right in each pair of the trace columns) 15 min during Day 1 and Day 5 IVSA sessions in saline (**A**) and cocaine (**B**) mice.

C-F, Ca^{2+} transient amplitude ΔZ based-classification of each 30-sec block of M2 neurons within 3 min after RNF in the first *vs*. the last 15 min during Day 1 and Day 5 IVSA sessions in saline (**C**) and cocaine (**E**) mice. The proportions of M2 neurons in each category in a 15-min session are summarized in **D** for saline mice and **F** for cocaine mice.

Figure S7. **Overlaps of IVSA event-associated LANs in M2.**

Figure 1

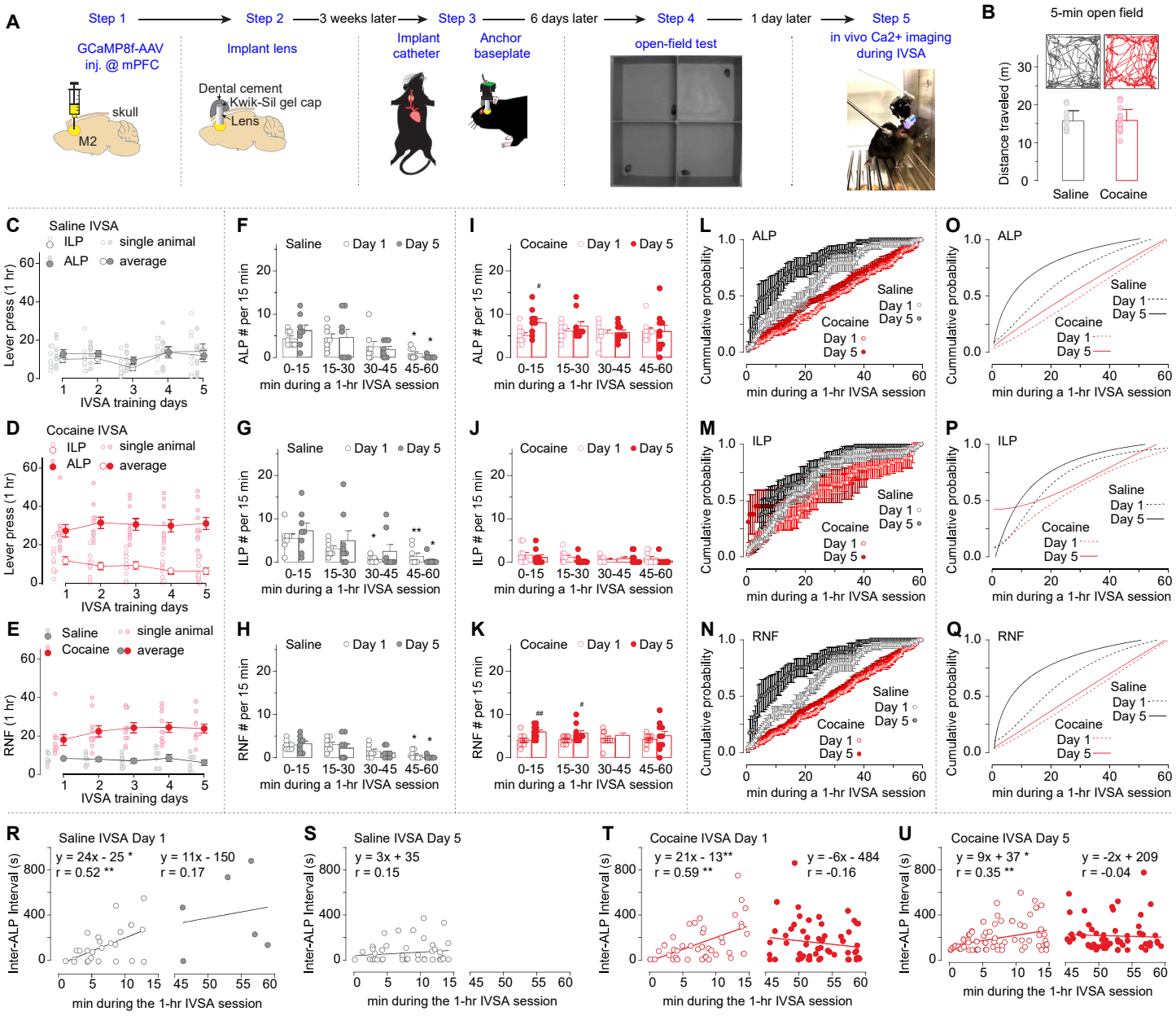
A
Step 1
Step 2
3 weeks later
Step 3
6 days later
Step 4
1 day later
Step 5
GCaMP8f-AAV inj. @ mPFC
Implant lens
Implant catheter
Anchor baseplate
open-field test
in vivo Ca2+ imaging during IVSA
skull
M2
Dental cement
Kwik-Sil gel cap
Lens
B
5-min open field
Distance traveled (m)
Saline
Cocaine
C
Saline IVSA
ILP
single animal
ALP
average
Lever press (1 hr)
IVSA training days
D
Cocaine IVSA
E
Saline
Cocaine
RNF (1 hr)
F
ALP # per 15 min
min during a 1-hr IVSA session
G
ILP # per 15 min
H
RNF # per 15 min
I
J
K
L
ALP
Cumulative probability
M
ILP
N
RNF
O
P
Q
R
Saline IVSA Day 1
y = 24x - 25 *
r = 0.52 **
y = 11x - 150
r = 0.17
Inter-ALP Interval (s)
min during the 1-hr IVSA session
S
Saline IVSA Day 5
y = 3x + 35
r = 0.15
T
Cocaine IVSA Day 1
y = 21x - 13**
r = 0.59 **
y = -6x - 484
r = -0.16
U
Cocaine IVSA Day 5
y = 9x + 37 *
r = 0.35 **
y = -2x + 209
r = -0.04

Figure 2

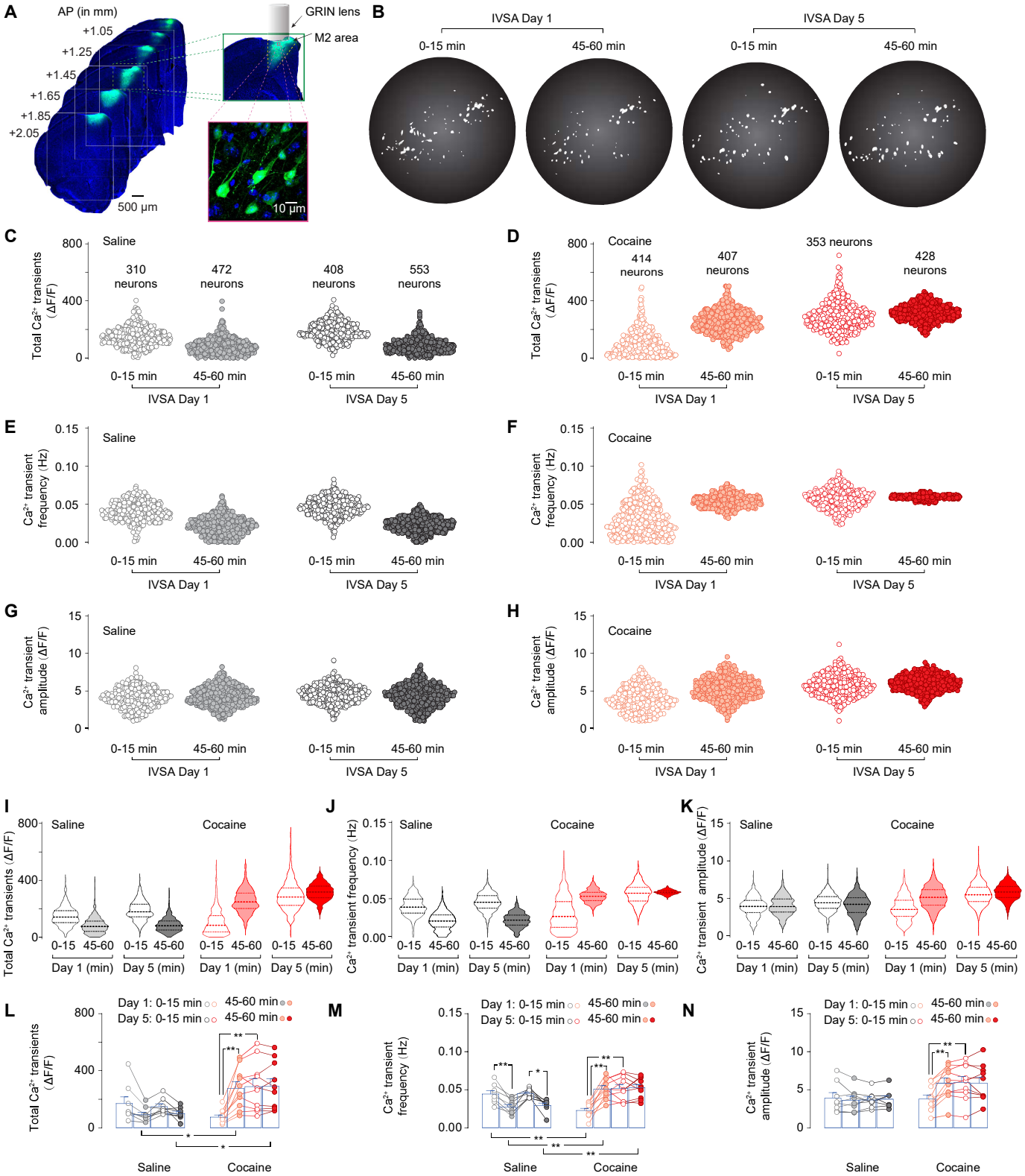
A
AP (in mm)
+1.05
+1.25
+1.45
+1.65
+1.85
+2.05
500 µm
GRIN lens
M2 area
10 µm
B
IVSA Day 1
IVSA Day 5
0-15 min
45-60 min
C
Saline
310 neurons
472 neurons
408 neurons
553 neurons
Total Ca2+ transients (ΔF/F)
D
Cocaine
414 neurons
407 neurons
353 neurons
428 neurons
E
Ca2+ transient frequency (Hz)
F
G
Ca2+ transient amplitude (ΔF/F)
H
I
Day 1 (min)
Day 5 (min)
J
K
L
Day 1: 0-15 min
Day 5: 0-15 min
M
N

Figure 3

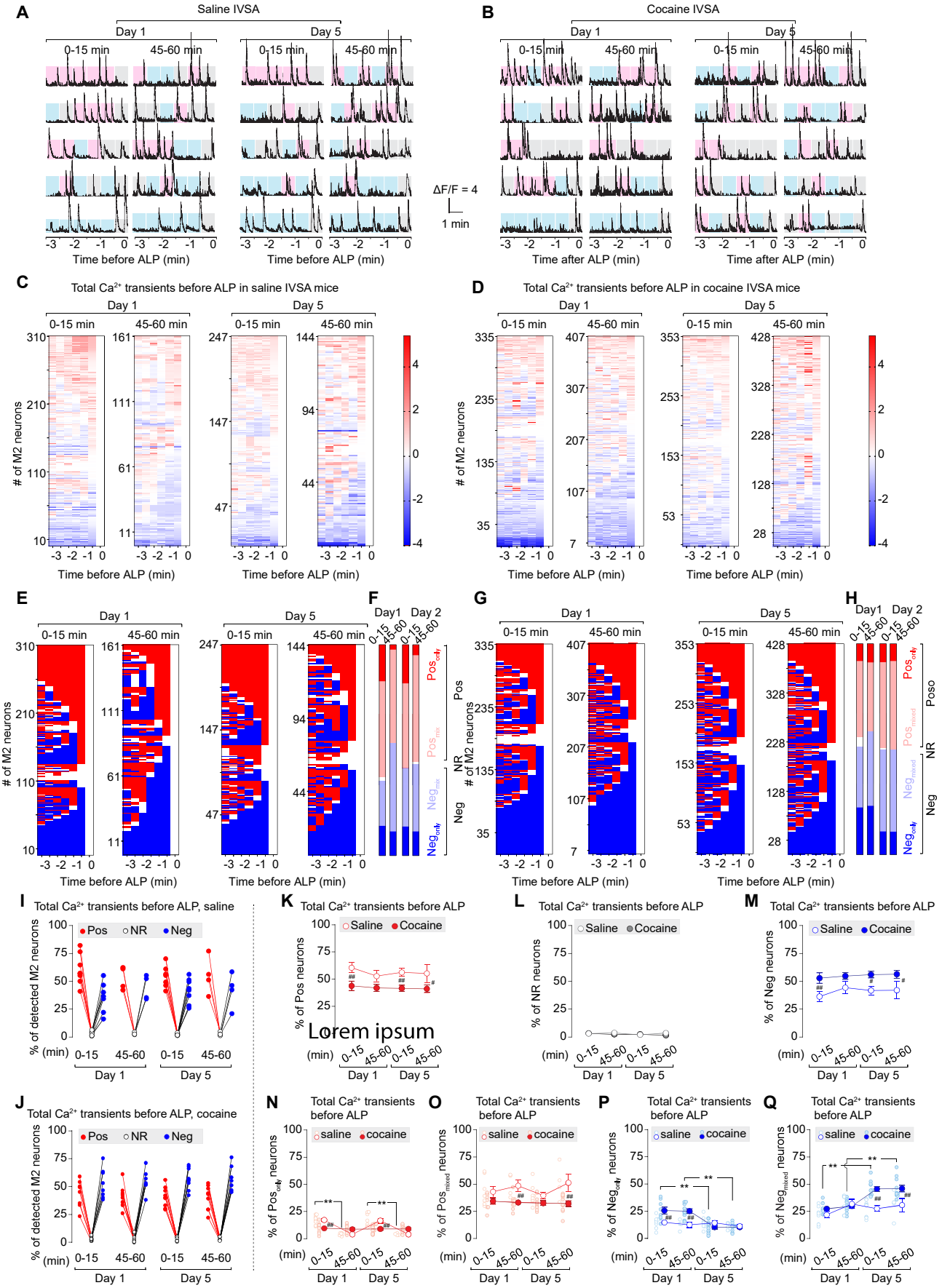
A
Saline IVSA
Day 1
Day 5
0-15 min
45-60 min
ΔF/F = 4
1 min
Time before ALP (min)
B
Cocaine IVSA
Time after ALP (min)
C
Total Ca2+ transients before ALP in saline IVSA mice
# of M2 neurons
D
Total Ca2+ transients before ALP in cocaine IVSA mice
E
F
Day1
Day 2
Pos
NR
Neg
G
H
I
Total Ca2+ transients before ALP, saline
% of detected M2 neurons
Pos
NR
Neg
(min)
J
Total Ca2+ transients before ALP, cocaine
K
Total Ca2+ transients before ALP
Saline
Cocaine
% of Pos neurons
Lorem ipsum
L
% of NR neurons
M
% of Neg neurons
N
saline
cocaine
O
P
Q

Figure 4

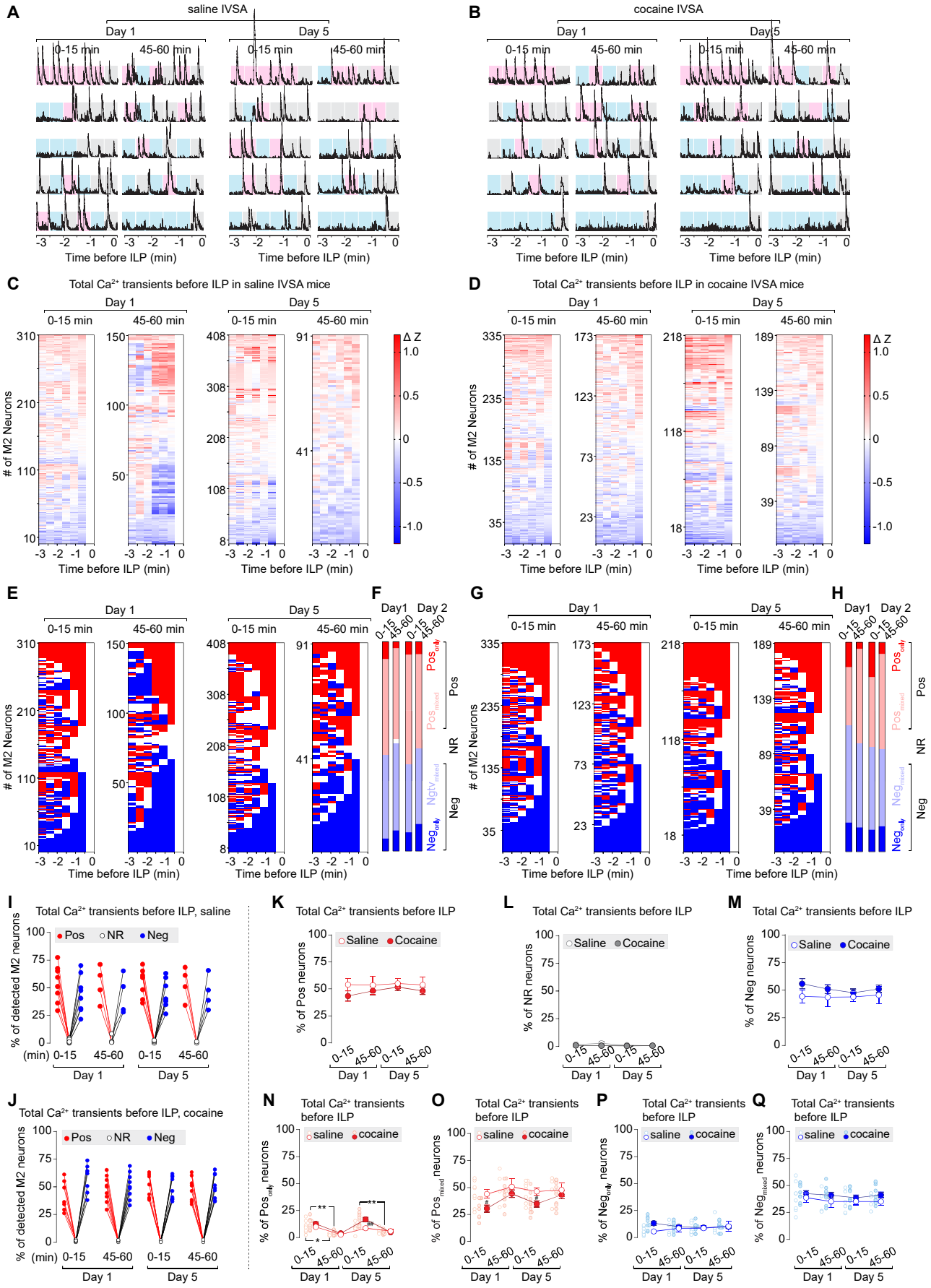
A
saline IVSA
Day 1
Day 5
0-15 min
45-60 min
Time before ILP (min)
B
cocaine IVSA
C
Total Ca2+ transients before ILP in saline IVSA mice
# of M2 Neurons
Δ Z
D
Total Ca2+ transients before ILP in cocaine IVSA mice
E
F
Day1
Day 2
Pos
NR
Neg
G
H
I
Total Ca2+ transients before ILP, saline
% of detected M2 neurons
Pos
NR
Neg
(min)
J
Total Ca2+ transients before ILP, cocaine
K
Total Ca2+ transients before ILP
% of Pos neurons
Saline
Cocaine
L
% of NR neurons
M
% of Neg neurons
N
% of Pos only neurons
saline
cocaine
O
% of Pos mixed neurons
P
% of Neg only neurons
Q
% of Neg mixed neurons

Figure 5

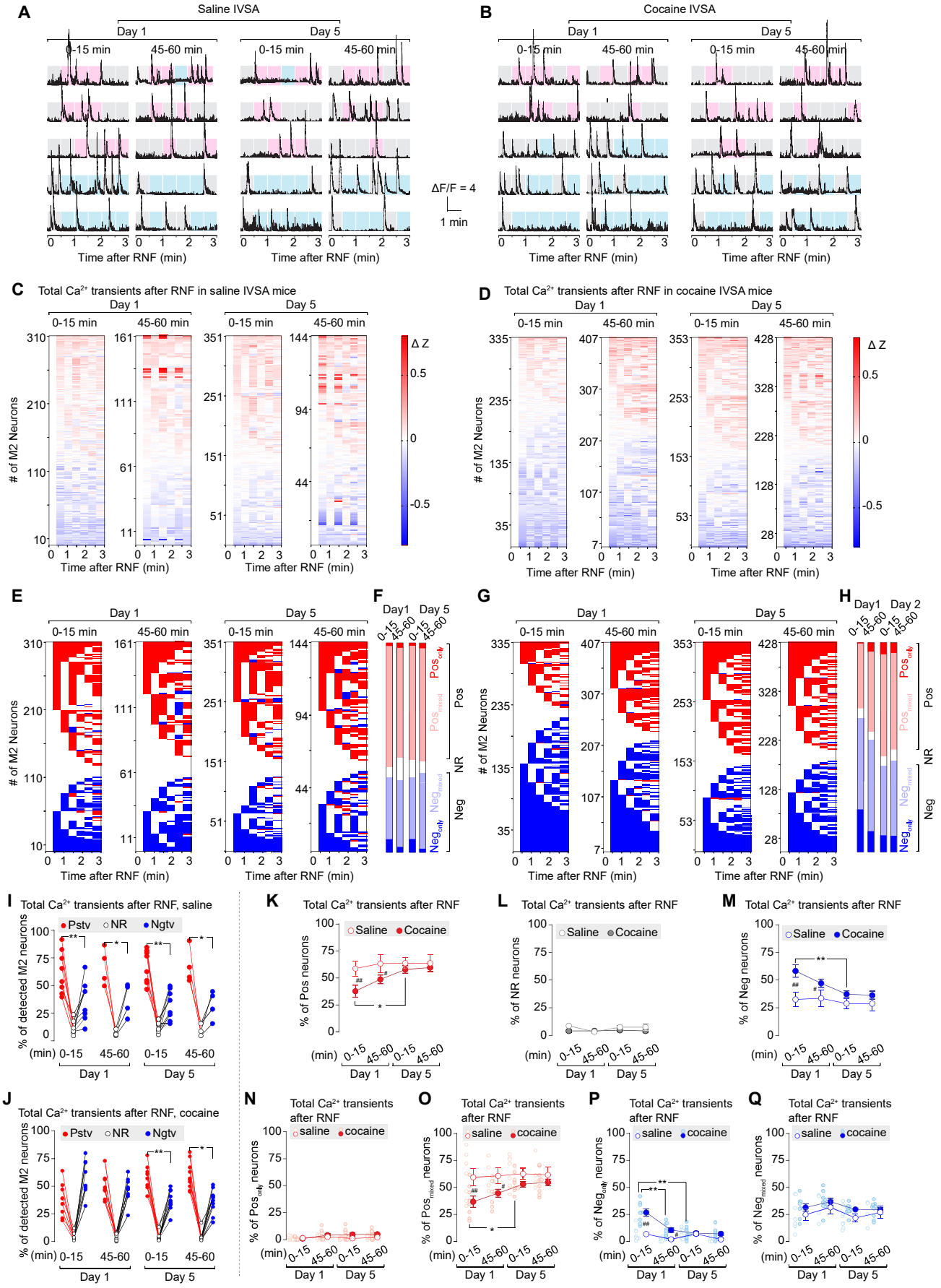
A
Saline IVSA
Day 1
Day 5
0-15 min
45-60 min
ΔF/F = 4
1 min
Time after RNF (min)
B
Cocaine IVSA
C
Total Ca2+ transients after RNF in saline IVSA mice
# of M2 Neurons
Δ Z
D
Total Ca2+ transients after RNF in cocaine IVSA mice
E
F
Day1
Day 5
Pos
NR
Neg
G
H
Day 2
I
Total Ca2+ transients after RNF, saline
% of detected M2 neurons
Pstv
NR
Ngtv
(min)
J
Total Ca2+ transients after RNF, cocaine
K
Total Ca2+ transients after RNF
% of Pos neurons
Saline
Cocaine
L
% of NR neurons
M
% of Neg neurons
N
% of Pos neurons
saline
cocaine
O
P
% of Neg neurons
Q

Figure 6

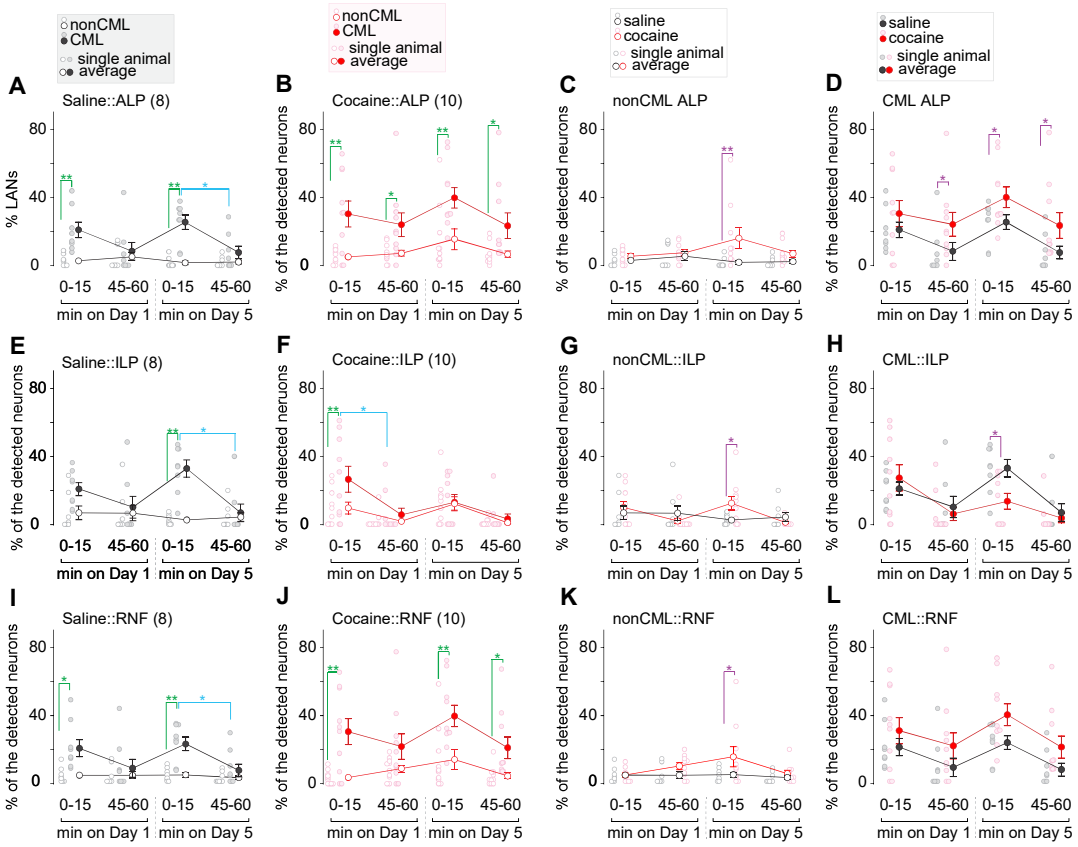
nonCML
CML
single animal
average
A
Saline::ALP (8)
% LANs
B
Cocaine::ALP (10)
% of the detected neurons
saline
cocaine
C
nonCML ALP
D
CML ALP
E
Saline::ILP (8)
F
Cocaine::ILP (10)
G
nonCML::ILP
H
CML::ILP
I
Saline::RNF (8)
J
Cocaine::RNF (10)
K
nonCML::RNF
L
CML::RNF
0-15
45-60
min on Day 1
min on Day 5

Figure 7

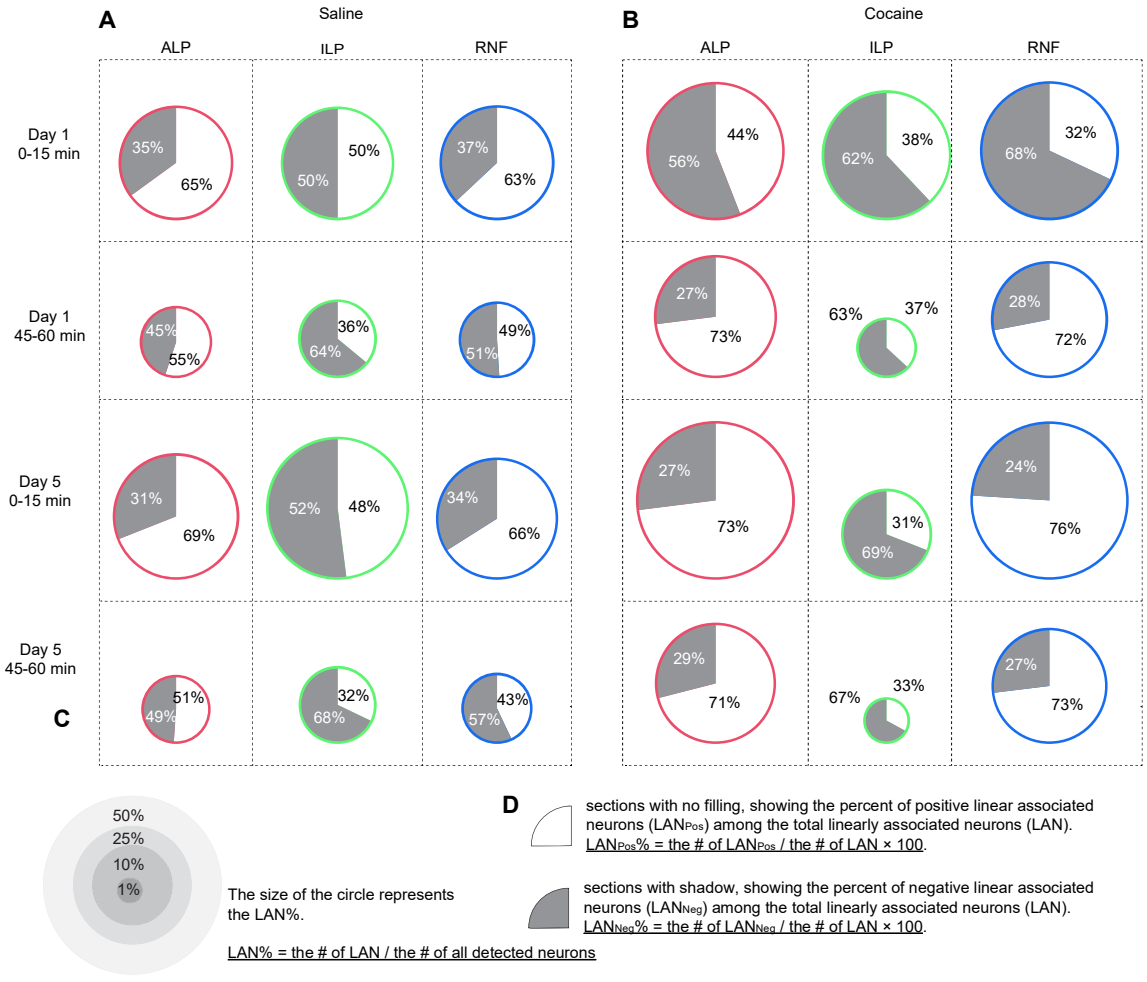
A
Saline
ALP
ILP
RNF
B
Cocaine
ALP
ILP
RNF
Day 1
0-15 min
35%
65%
50%
50%
37%
63%
56%
44%
62%
38%
68%
32%
Day 1
45-60 min
45%
55%
36%
64%
49%
51%
27%
73%
63%
37%
28%
72%
Day 5
0-15 min
31%
69%
52%
48%
34%
66%
27%
73%
31%
69%
24%
76%
Day 5
45-60 min
C
51%
49%
32%
68%
43%
57%
29%
71%
67%
33%
27%
73%
50%
25%
10%
1%
The size of the circle represents the LAN%.
LAN% = the # of LAN / the # of all detected neurons
D
sections with no filling, showing the percent of positive linear associated neurons (LANPos) among the total linearly associated neurons (LAN).
LANPos% = the # of LANPos / the # of LAN × 100.
sections with shadow, showing the percent of negative linear associated neurons (LANNeg) among the total linearly associated neurons (LAN).
LANNeg% = the # of LANNeg / the # of LAN × 100.

Figure 8

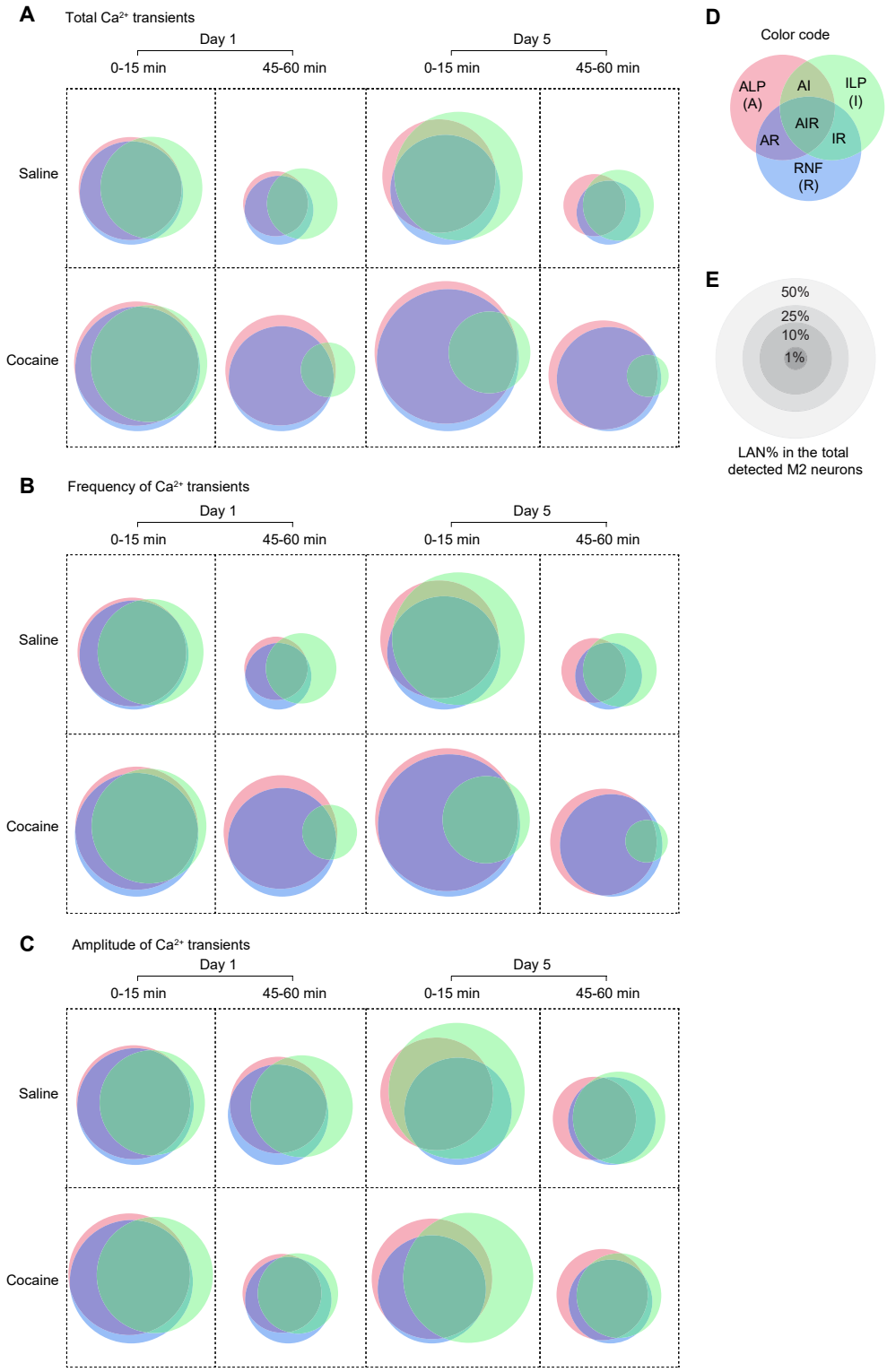
A
Total Ca²⁺ transients
Day 1
Day 5
0-15 min
45-60 min
0-15 min
45-60 min
Saline
Cocaine
B
Frequency of Ca²⁺ transients
Day 1
Day 5
0-15 min
45-60 min
0-15 min
45-60 min
Saline
Cocaine
C
Amplitude of Ca²⁺ transients
Day 1
Day 5
0-15 min
45-60 min
0-15 min
45-60 min
Saline
Cocaine
D
Color code
ALP
(A)
AI
ILP
(I)
AIR
AR
IR
RNF
(R)
E
50%
25%
10%
1%
LAN% in the total
detected M2 neurons

Figure S1

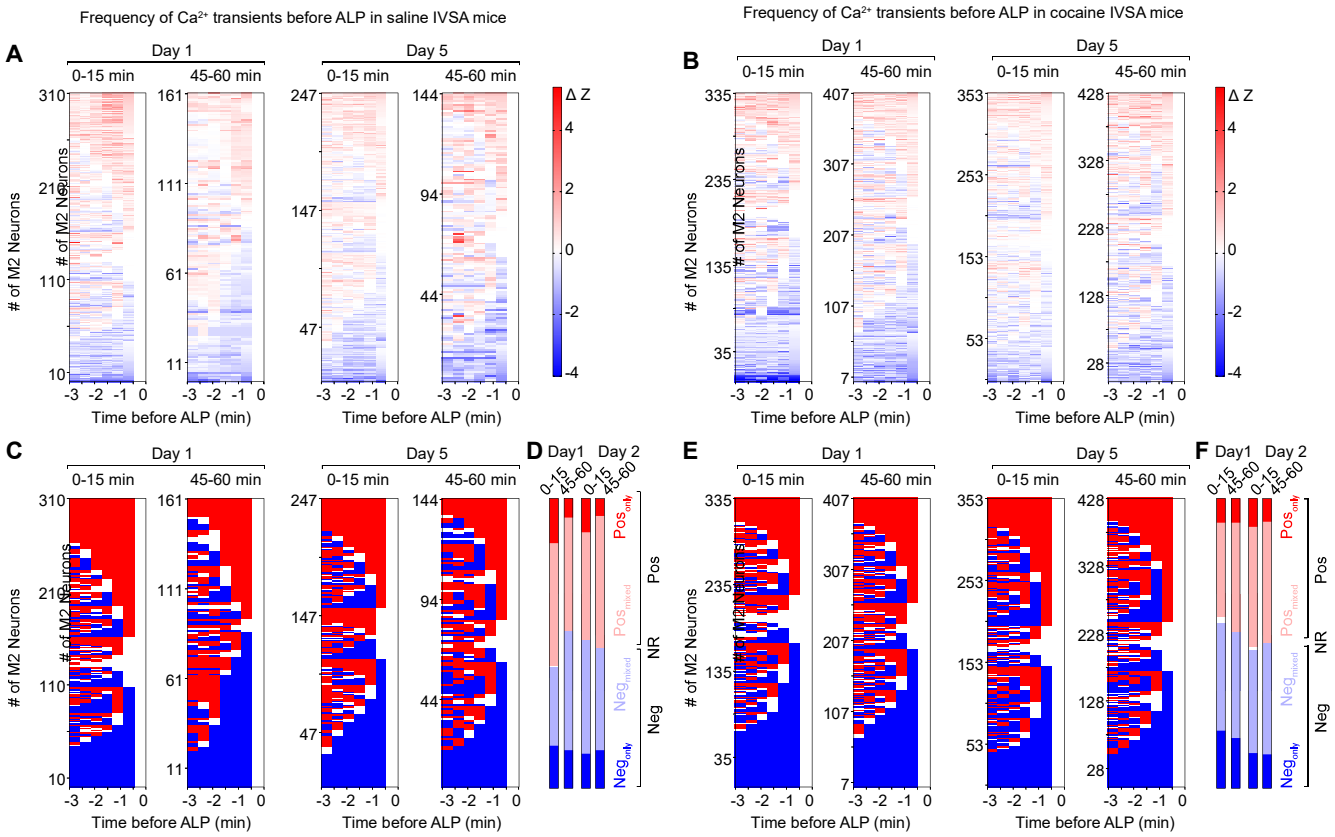

Figure S2

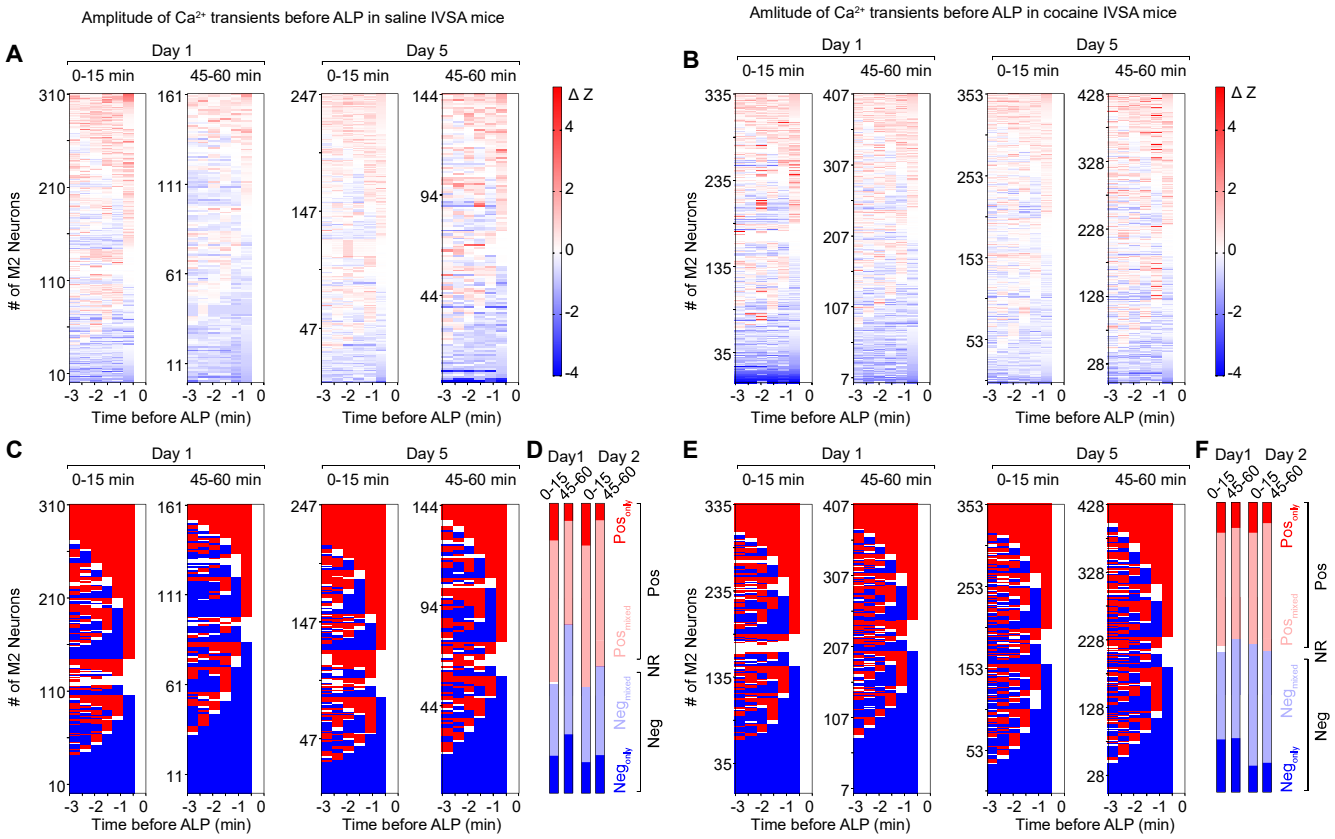

Figure S3

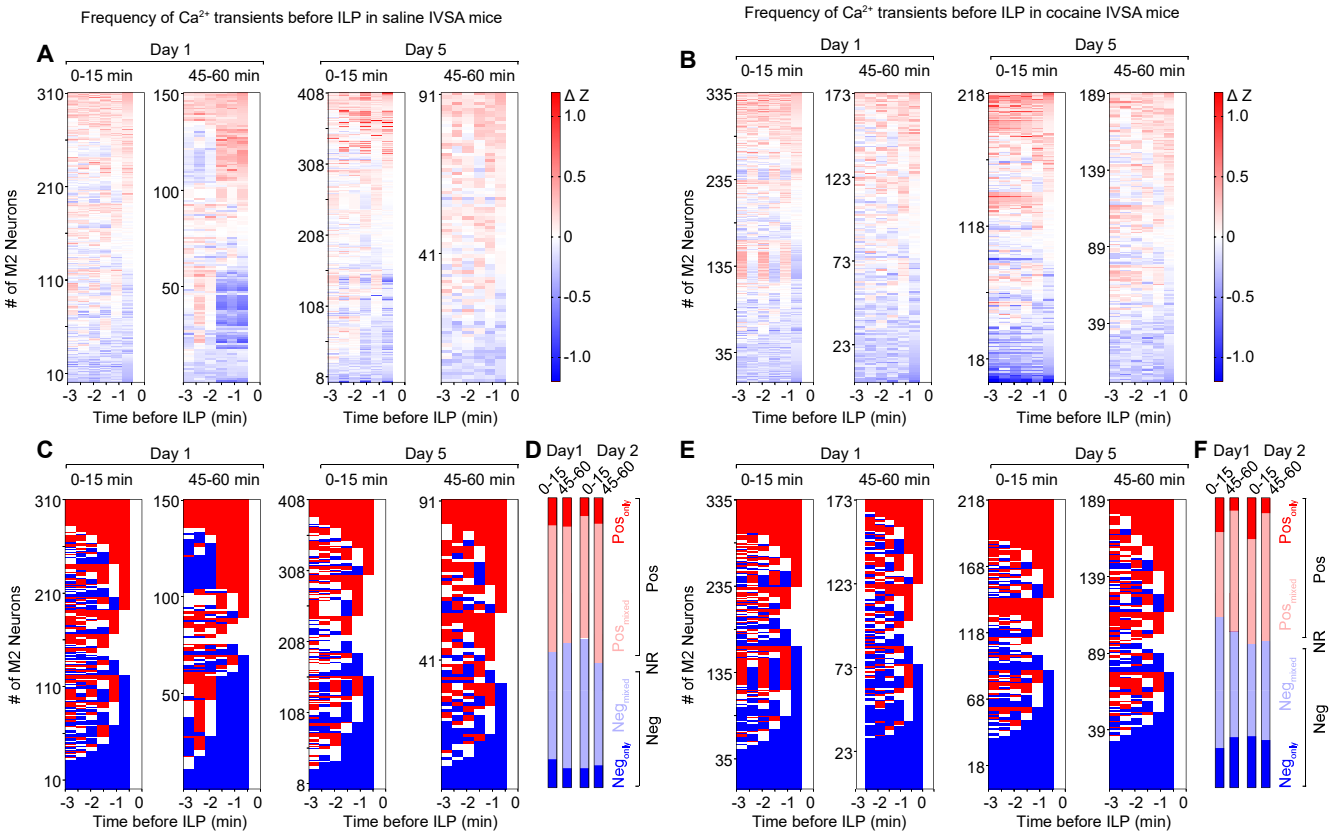

Figure S4

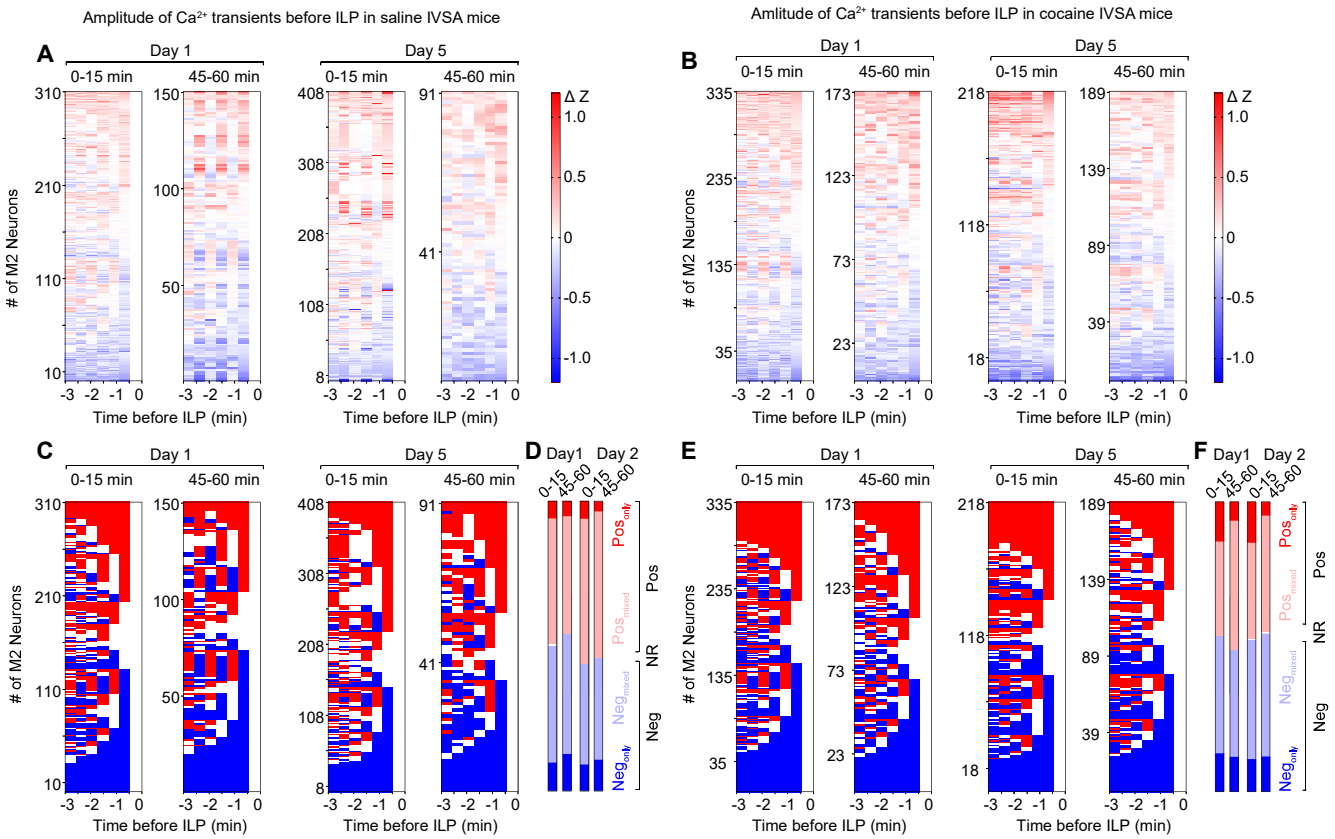

Figure S5

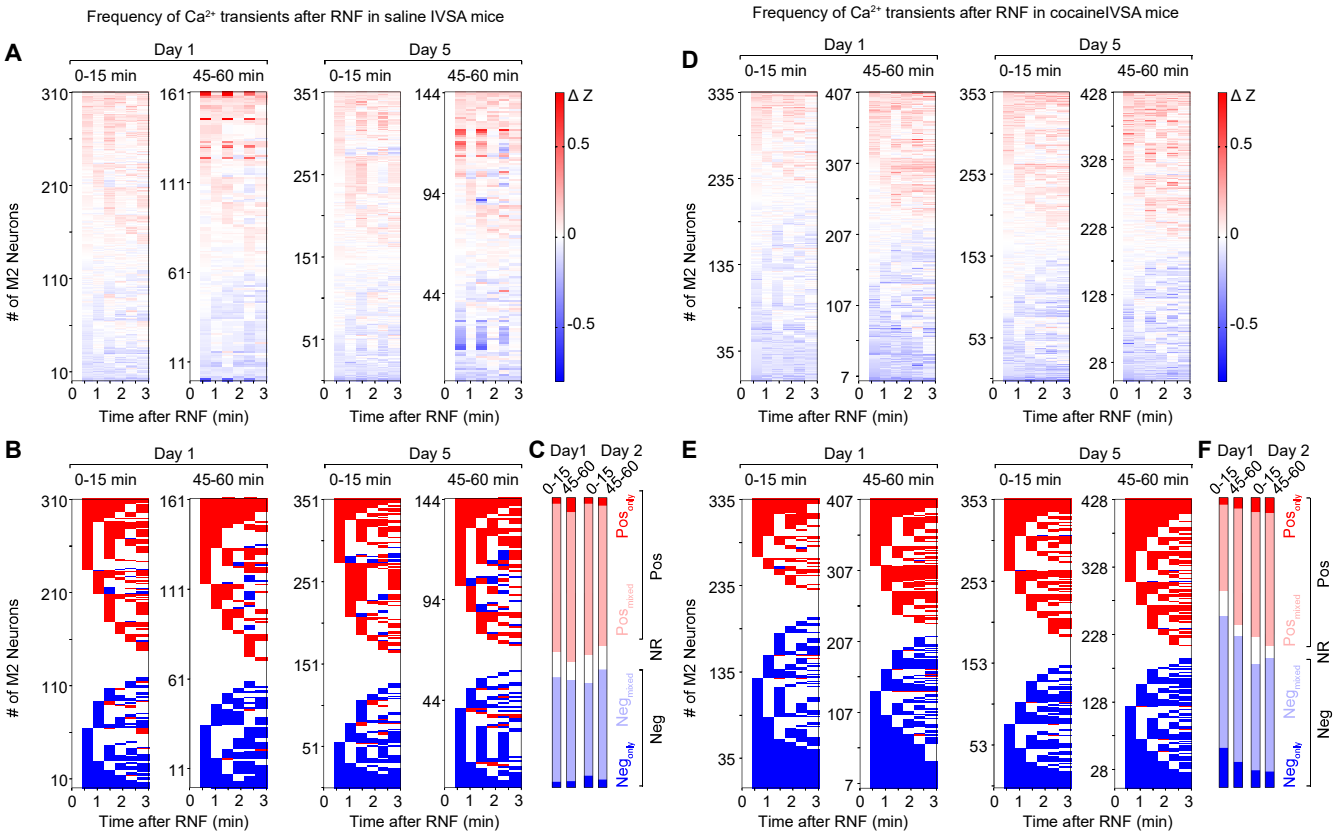

Figure S6

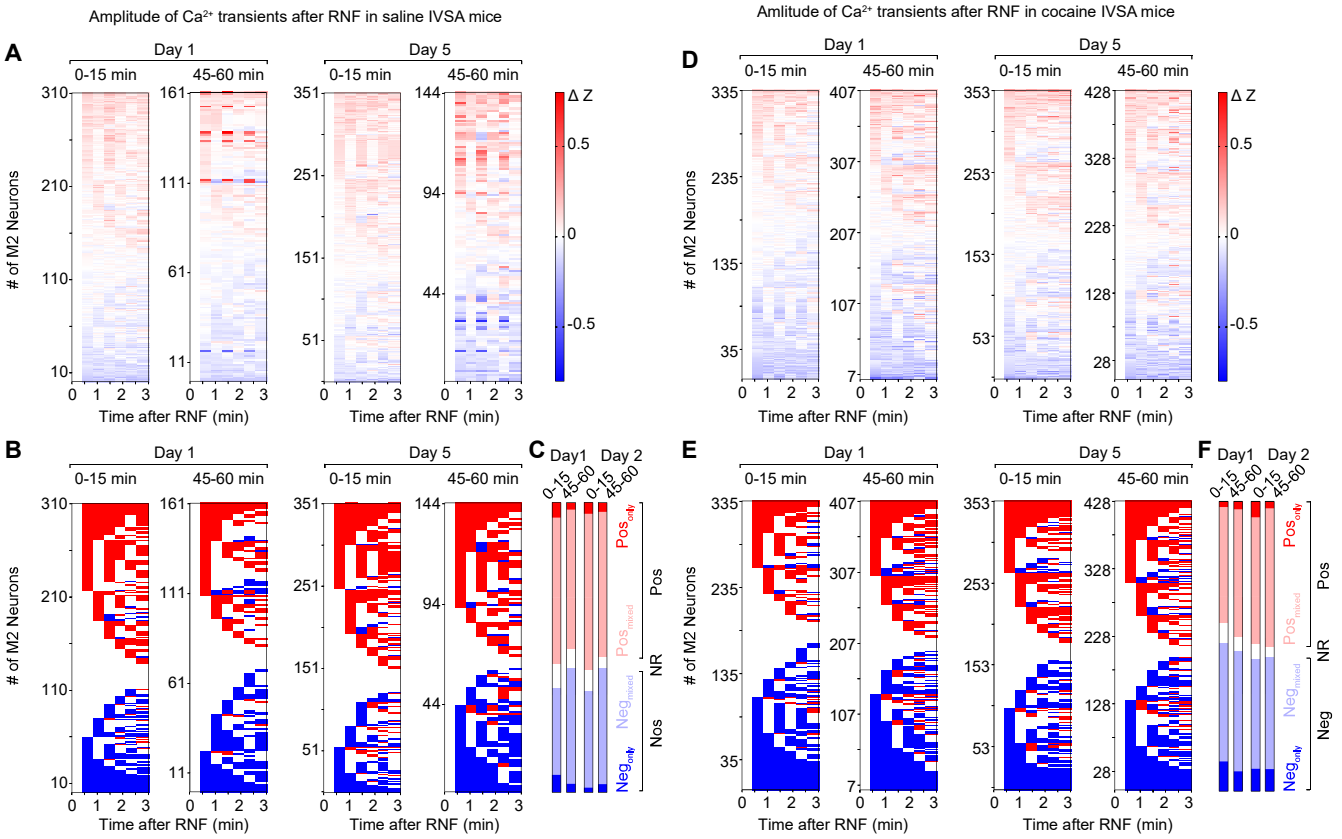

Figure S7

Saline:: ALP LANs
Cocaine::ALP LANs
Saline:: IALP LANs
Cocaine::IALP LANs
Saline:: RNF LANs
Cocaine::RNF LANs
Day 1
0-15 min
45-60 min
Day 5
0-15 min
45-60 min
A
AI
AR
AIR
I
AI
IR
AIR
R
AR
IR
AIR
Color code
ALP
(A)
AI
ILP
(I)
AIR
AR
IR
RNF
(R)